WT MV no longer entered EMT-induced II-18 cells, which suggests that the epithelial cell receptor is down-regulated by the induction of EMT. Other polarized cell lines, NCI-H358 and HT-29, also lost susceptibility to WT MV when EMT was induced. However, the complete formation of tight junctions rather reduced MV entry into HT-29 cells. Taken together, these data suggest that the unidentified epithelial cell receptor for MV may be involved in the formation of epithelial intercellular junctions.

EXPERIMENTAL PROCEDURES

Cells—II-18 cells (RCB2093, Riken Bioresource Center Cell Bank (Tsukuba, Japan)) were maintained in RPMI medium (ICN Biomedicals (Aurora, OH)) supplemented with 7.5% fetal bovine serum (FBS). PLAT-gp cells, kindly provided by M. Shimojima and T. Kitamura, are retrovirus-packaging cells, which contain the retroviral *gag* and *pol* genes (28). PLAT-gp cells were maintained in Dulbecco's modified Eagle's medium (DMEM; Invitrogen) supplemented with 7.5% FBS and 10 μg/ml blasticidin (InvivoGen (San Diego, CA)). The characteristics and culture conditions used for the following cell lines were as described previously: Vero/hSLAM (29), NCI-H358 (30), HT-29 (31), and A549 (32).

Viruses—All full-length genome plasmids were derived from the p(+)MV323 plasmid encoding the antigenomic full-length cDNA of the IC-B WT strain of MV (33). The p(+)MV323-EGFP and p(+)MV323-Luci plasmids, which contain an additional transcriptional unit of enhanced green fluorescent protein (EGFP) and the *Renilla* luciferase gene, respectively, were reported previously (14, 34). p(+)MV/Ed-H-EGFP and p(+)MV/Ed-H-Luci contain the Edmonston tag H gene in place of the IC-B WT H gene (14, 35). p(+)MV323/H(Y543S)-EGFP has a mutation in the H gene resulting in the amino acid substitution Y543S; the mutant H protein is incapable of interacting with the putative epithelial cell receptor (15). Recombinant MV strains generated from p(+)MV323-EGFP, p(+)MV323-Luci, p(+)MV/Ed-H-EGFP, p(+)MV/Ed-H-Luci, and p(+)MV323/H(Y543S)-EGFP were named IC323-EGFP, IC323-Luci, IC323/Ed-H-EGFP, IC323/Ed-H-Luci, and IC323/H(Y543S)-EGFP, respectively. They were generated as reported previously (36, 37).

Plasmid Constructions—pCVSV-G is an expression plasmid that was made by cloning a cDNA encoding the vesicular stomatitis virus G protein into the expression vector pCAGGS (38). pMX-GFP, kindly provided by M. Shimojima and T. Kitamura, is a plasmid for a Moloney murine leukemia virus-based retrovirus vector expressing GFP (39, 40). pMXs-IP is a plasmid for a retrovirus vector with multiple cloning sites (41). To generate a plasmid for a retrovirus vector expressing Snail, total RNA was extracted from A549 cells, the cDNA encoding Snail was amplified by reverse transcription and PCR, and pMXs-IP-Snail was generated by inserting Snail cDNA into the EcoRI and NotI sites of pMXs-IP. The eukaryotic expression vectors pCA7 (36, 42) and pCA7ps (15) are derivatives of pCAGGS (38). pCA7ps-ICH, pCA7ps-EdH, and pCA7-ICF, which encode the IC-B H protein, the Edmonston tag H protein, and the IC-B F protein, respectively (15, 35), have been described previously.

Retrovirus Vector—PLAT-gp cells were cultured in collagen-coated 6-well cluster plates (Iwaki Glass Co. Ltd., Chiba, Japan). pMX-GFP (4 μg), pMXs-IP (4 μg), or pMXs-IP-Snail (4 μg) was transfected, together with pCVSV-G (0.4 μg), into PLAT-gp cells, using Lipofectamine 2000 (Invitrogen). After 2 or 3 days posttransfection, supernatant was harvested and filtered through a 0.45-μm filter (Millipore, Bedford, MA). The retrovirus vector expressing GFP (MX-GFP) was used for titration. II-18 cells were cultured in collagen-coated 48-well cluster plates (Corning Glass) and infected by serially diluted MX-GFP. After 48 h postinfection (p.i.), the number of GFP-expressing cells was counted under a fluorescence microscope. Cells were infected with the retrovirus vector expressing Snail in medium containing 4 μg/ml Polybrene at a multiplicity of infection (MOI) of 50–100. A retrovirus vector derived from pMXs-IP was used for control experiments.

FACS Analysis—Cells were harvested and fixed with phosphate-buffered saline (PBS) containing 4% paraformaldehyde for 20 min at room temperature. After being washed with PBS, cells were permeabilized in PBS containing 0.05% Triton X-100 for 5 min at room temperature. Cells were then incubated with the mouse polyclonal antibody against Snail (Abnova (Taipei, Taiwan)) for 1 h on ice, followed by incubation with Alexa Fluor 488-conjugated anti-mouse secondary antibody (Molecular Probes, Inc. (Eugene, OR)). Cells were analyzed by flow cytometry and ModFit software (version 3.0; Verity Software House).

Western Blot Analysis—Cells were lysed in a radioimmunoprecipitation assay buffer (150 mM NaCl, 10 mM Tris-HCl, pH 7.4, 1% Triton X-100, 1% sodium deoxycholate, 0.1% SDS), and polypeptides in cells were separated by SDS-PAGE and blotted onto polyvinylidene difluoride membranes (Hybond-P; Amersham Biosciences). The membranes were then incubated with primary antibodies for 16 h. A mouse monoclonal antibody (mAb) against E-cadherin (Invitrogen), occludin (Invitrogen), or actin (Santa Cruz Biotechnology, Inc. (Santa Cruz, CA)) and rabbit polyclonal antibody against claudin-1 (Invitrogen) or ZO-1 (Invitrogen) were used. The membranes were washed with Tris-buffered saline containing 0.05% Tween 20 and incubated with peroxidase-conjugated goat anti-mouse (Bio-Rad) or anti-rabbit IgG antibody (Zymed) for 1 h at room temperature. After membranes were washed with Tris-buffered saline, 0.05% Tween 20, they were treated with the ECL Plus reagent (Amersham Biosciences), and chemiluminescent signals were detected and visualized using a VersaDoc 3000 imager (Bio-Rad).

Immunofluorescence Staining and Confocal Microscopy—Cells were cultured on 35-mm Petri dishes with thin bottoms (μ-Dish 35 mm, high; Ibidi (Munich, Germany)) or on collagen-coated coverslips. After the treatments described in the respective procedures, cells were fixed and permeabilized with PBS containing 2.5% formaldehyde and 0.5% Triton X-100. Cells were then washed with PBS and incubated with a mAb against ZO-1 (Invitrogen) or E-cadherin (Invitrogen) for 1 h at 37 °C, followed by incubation with Alexa Fluor 488-conjugated anti-mouse secondary antibody (Molecular Probes). Nuclear DNA was stained with propidium iodide (Sigma) at 10 μg/ml. Images of cells were obtained sequentially from the top to the bottom of the cells by using a confocal microscope (Radiance

2100, Bio-Rad) and merged together by using Lasersharp software (Bio-Rad).

cDNA Microarray Analysis—Total RNA was isolated from cells using the RNeasy Plus Mini kit (Qiagen (Valencia, CA)). RNA was amplified and labeled using the Illumina TotalPrep RNA Amplification Kit (Ambion, Austin, TX). HumanWG-6 version 3.0 BeadChip (Illumina, Hayward, CA) was hybridized with labeled cRNA. Data were submitted to the GEO database, accession number GSE19679, and analyzed using BeadStudio (Illumina) and KeyMolnet software (IMMD Inc., Tokyo, Japan).

Virus Titration—Monolayers of Vero/hSLAM cells on 12-well cluster plates were infected with serially diluted virus samples and incubated for 1 h at 37 °C. After being washed with PBS, the cells were overlaid with DMEM containing 7.5% FBS and 1% methylcellulose. At 4 days p.i., the titers of EGFP-expressing viruses were determined by counting the numbers of plaques under a fluorescence microscope. The number of plaques of luciferase-expressing viruses was counted after neutral red staining. Cell infectious units (CIU) of EGFP-expressing viruses were also determined as described previously (34, 42).

Virus Growth—II-18 cells cultured in 12-well cluster plates were infected with IC323-EGFP at an MOI of 0.01. At various days p.i., both cells and media were collected to determine the titers in them.

Measurement of Infectivity—Cells were cultured in collagen-coated 48-well cluster plates (Corning Glass). After the treatments described in the respective procedures, cells were incubated by *Renilla* luciferase-expressing MVs at an MOI of 0.01. After 3 h p.i., DMEM supplemented with 7.5% FBS and 100 μg/ml fusion block peptide (Z-D-Phe-Phe-Gly) (43) (Peptide Institute Inc. (Osaka, Japan)) was added to each well to block the second round of infection by progeny viruses. After 24 h p.i., cells were lysed in the *Renilla* luciferase assay lysis buffer. The *Renilla* luciferase activity in the cells was then analyzed using a *Renilla* luciferase assay system (Promega (Madison, WI)), according to the manufacturer's instructions. Chemiluminescence was measured using a Mithras LB940 plate reader (Berthold Technologies (Pforzheim, Germany)). Luciferase activity of control samples was set to 100% in each experiment.

Fusion Assay—CHO cells cultured in 6-well cluster plates were cotransfected with pCA7ps-ICH or pCA7ps-EdH (2 μg) plus pCA7-ICF (2 μg), using Lipofectamine 2000 (Invitrogen). Two days after transfection, the cells were cocultured with II-18 cells. After 2 days of incubation, the cells were observed after Giemsa staining under a light microscope.

Modulation of the Tight Junction Formation—HT-29 cells were seeded at 15% confluence on collagen-coated coverslips or 6-well plates. At various time intervals (1, 3, 10, and 16 days after plating), cells were used for virus infection or immunostaining. Alternatively, the culture media of HT-29 cells 8–12 days after plating were changed to calcium-free media (Invitrogen) or DMEM (Invitrogen). After 24 h, cells were used for virus infection or immunostaining. After virus infection, DMEM supplemented with 7.5% FBS and 100 μg/ml fusion block peptide was added to each well. At 36 h p.i., the number of EGFP-expressing cells was counted under a fluorescence microscope.

RESULTS

SLAM- and CD46-independent MV Infection of II-18 Cells—WT MV infects and replicates in polarized epithelial cell lines, such as NCI-H358, HT-29, Calu-3, Caco-2, and T84 (14, 15). However, these cell lines are not as easy to propagate as other common cell lines because of their slow growth and a requirement for special medium. After screening many cell lines, we found that a human lung adenocarcinoma cell line, II-18, is not only highly susceptible to WT MV but also grows fast in RPMI medium.

To examine whether MV infects II-18 cells in a SLAM-independent manner, II-18 and Vero/hSLAM cells were infected with IC323-Luci, a recombinant virus encoding a reporter luciferase based on a WT strain of MV, in medium containing a mAb against SLAM (IPO-3) (44) (Kamiya Biomedical (Seattle, WA)) or mouse control IgG. IPO-3 prevented IC323-Luci entry into Vero/hSLAM cells but not II-18 cells (Fig. 1*A*). An epithelial cell receptor-blind MV IC323/H(Y543S)-EGFP, which has a Y543S substitution on the receptor-binding H protein and cannot utilize the epithelial cell receptor, was reported previously (15). II-18 cells were infected with IC323-EGFP and IC323/H(Y543S)-EGFP and observed under a fluorescence microscope at 2 days p.i. Infection with IC323-EGFP induced syncytium formation in II-18 cells, whereas infection with IC323/H(Y543S)-EGFP did not (Fig. 1*B*). WT MV does not use CD46 as a receptor. All of these results indicate that MV infects II-18 cells in a SLAM- and CD46-independent manner. The infectious titer of the same stock of IC323-EGFP was measured in Vero/SLAM, II-18, NCI-H358, and HT-29 cells. The titer in II-18 cells was comparable with that in Vero/SLAM cells (Fig. 1*C*), indicating that WT MV infects II-18 and SLAM-positive cells at almost the same efficiency. The titers in NCI-H358 and HT-29 cells were much lower than that in II-18 cells. These data indicate that II-18 cells are suitable for studying an unidentified epithelial cell receptor. To investigate whether II-18 cells can support multiple cycles of MV growth, a growth curve of IC323-EGFP in II-18 cells was examined (Fig. 1*D*). Although II-18 cells supported multiple cycles of MV growth, the peak titer was lower than that in other polarized cell lines reported previously (14, 15). There may be postentry defects of MV replication in II-18 cells.

Destruction of Adherens and Tight Junctions in II-18 Cells by Snail Expression—Snail is a transcriptional repressor that induces EMT (17). EMT-induced cells lose epithelial intercellular junctions, such as adherens and tight junctions (21, 22). To examine whether MV infection via the epithelial cell receptor is influenced by EMT, II-18 cells were infected with the retrovirus vector expressing Snail at an MOI of 50–100. Expression of Snail was confirmed by fluorescence-activated cell sorting analysis (Fig. 2*A*). After 2 days p.i., the morphology of II-18 cells was observed under a phase-contrast imaging microscope. II-18 cells expressing Snail seemed to have weak contacts with each other as compared with control cells (Fig. 2*B*). After 5 days p.i., expression of E-cadherin, occludin, claudin-1, and ZO-1 was examined by Western blot analysis. E-cadherin is a component of the adherens junction, and occludin, claudin-1, and ZO-1 are components of the

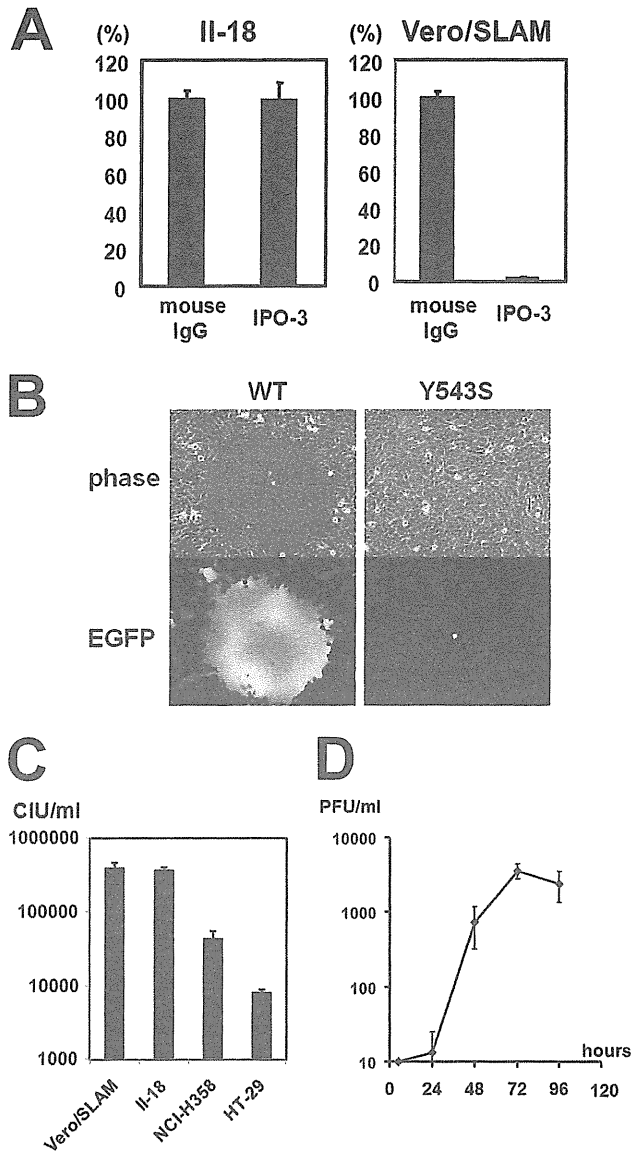

FIGURE 1. **SLAM-independent WT MV infection of II-18 cells.** *A*, monolayers of II-18 and Vero/hSLAM cells were incubated with medium containing control mouse IgG or IPO3 (anti-SLAM mAb) and infected with IC323-Luci at an MOI of 0.01. At 3 h p.i., the fusion block peptide was added to medium, and at 24 h p.i., the *Renilla* luciferase activity was measured. The activity in cells treated with control mouse IgG was set to 100%. *B*, monolayers of II-18 cells were infected with IC323-EGFP or IC323/H(Y543S)-EGFP. At 2 days p.i., the monolayers were observed under a phase-contrast or fluorescence microscope. *C*, monolayers of Vero/hSLAM, II-18, NCI-H358, and HT-29 cells were infected with serially diluted virus samples of the same stock of IC323-EGFP. Titers were measured by counting the numbers of EGFP-expressing cells under a fluorescence microscope. *D*, monolayers of II-18 cells were infected with IC323-EGFP at an MOI of 0.01. At various days p.i., virus was harvested, and its plaque-forming units were measured in Vero/hSLAM cells. *Error bars*, S.D.

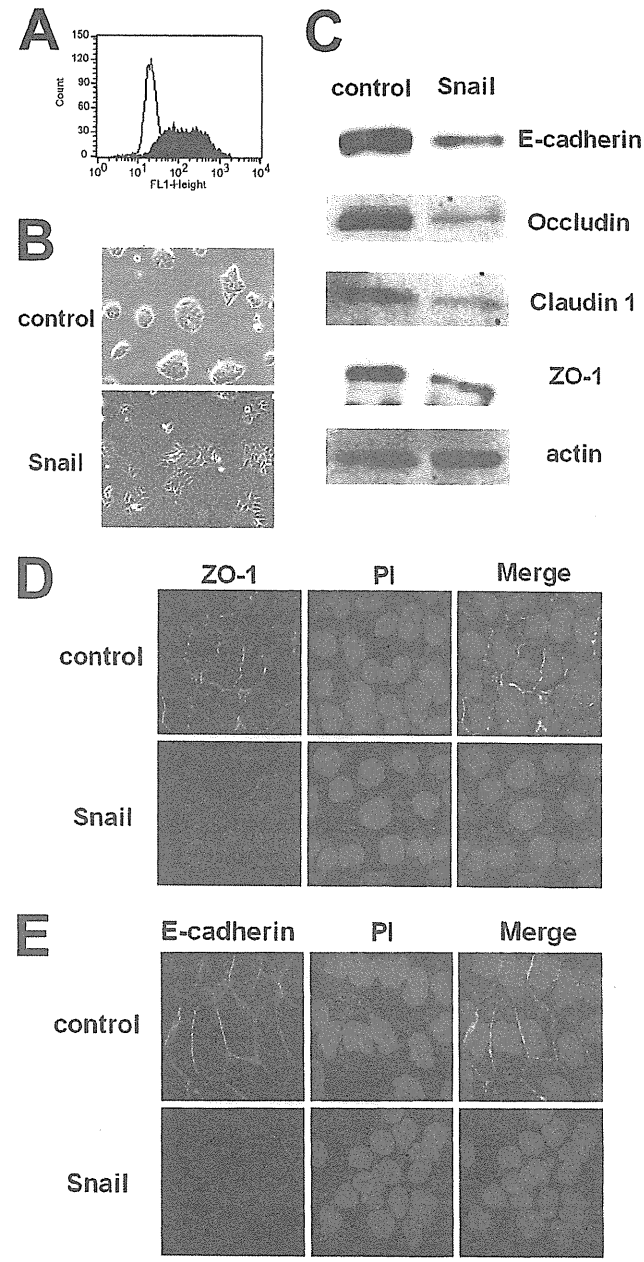

FIGURE 2. **Induction of EMT in II-18 cells by expressing Snail.** *A*, II-18 cells were infected with the retrovirus vector expressing Snail or control vector at an MOI of 50–100. At 5 days p.i., fluorescence-activated cell sorting analysis was performed to detect the expression of Snail. The expression of Snail was detected by using mouse polyclonal antibody against Snail. The *empty profile* represents control II-18 cells, and the *solid profile* represents Snail-expressing II-18 cells. *B*, at 2 days p.i., control and Snail-expressing II-18 cells were observed under a phase-contrast microscope. *C*, at 5 days p.i., cells were harvested, and expressions of E-cadherin, occludin, claudin-1, ZO-1, and actin were detected by Western blot analysis. *D* and *E*, at 5 days p.i., cells were permeabilized, fixed, and stained with a mAb against ZO-1 (*D*) or E-cadherin (*E*), followed by incubation with Alexa Fluor 488-conjugated anti-mouse secondary antibody. Nuclear DNA was stained with propidium iodide (*PI*). The cells were observed using a confocal microscope.

tight junction. They are used as epithelial markers (17). All of these proteins were down-regulated in II-18 cells expressing Snail (Fig. 2*C*). To investigate whether the formation of adherens and tight junctions was affected by Snail expression in II-18 cells, immunofluorescence staining of E-cadherin and ZO-1 was performed. The immunofluorescent staining pattern of ZO-1 indicated that tight junctions were formed in control II-18 cells, but they were destroyed by Snail expression (Fig. 2*D*). Similarly, adherens junctions were formed between neighboring II-18 cells, but they were destroyed after the induction of

TABLE 1
Down-regulated genes related to cell junctions

Symbol	Definition	Snail/Control[a]
CEACAM6	Carcinoembryonic antigen-related cell adhesion molecule 6	0.05
CD9	CD9 molecule	0.34
CDH1	Cadherin 1, type 1, E-cadherin (epithelial)	0.37
CLDN3	Claudin 3	0.11
CLDN7	Claudin 7	0.21
CLDN8	Claudin 8	0.23/0.34[b]

[a] Signals in Snail-expressing cells divided by those in control cells.
[b] Down-regulated as examined with two different *CLDN8* probes.

TABLE 2
Up- or down-regulated genes related to endocytosis or protein trafficking

Symbol	Definition	Snail/Control[a]
Endocytosis		
Up-regulated		
CAV1	Caveolin 1, caveolae protein, 22 kDa	2.38
CTSL1	Cathepsin L1	2.26/2.20[b]
Down-regulated		
CST6	Cystatin E/M	0.20/0.25[c]
Protein trafficking		
Down-regulated		
RAB17	RAB17, member RAS oncogene family	0.20
RAB25	RAB25, member RAS oncogene family	0.24
RAB38	RAB38, member RAS oncogene family	0.29
RAB40C	RAB40C, member RAS oncogene family	0.29
RAB11FIP1	RAB11 family-interacting protein 1	0.41
MAL2	MAL, T-cell differentiation protein 2	0.23
MALL	MAL, T-cell differentiation protein-like	0.40
STX3	Syntaxin 3	0.40
SCIN	Scinderin	0.42
MYO5C	Myosin VC	0.45

[a] Signals in Snail-expressing cells divided by those in control cells.
[b] Up-regulated as examined with two different *CTSL1* probes.
[c] Down-regulated as examined with two different probes of *CST6*.

EMT (Fig. 2*E*). These results indicate that Snail expression causes II-18 cells to lose the epithelial phenotype.

Modulation of mRNA Transcription Levels in II-18 Cells by Snail—Next, microarray analysis was performed to comprehensively investigate the influence of Snail expression on mRNA levels in II-18 cells. II-18 cells were infected with the retrovirus vector expressing Snail or the control vector at an MOI of 50–100. After 5 days p.i., total RNA was isolated from control or Snail-expressing II-18 cells, amplified, and labeled (n = 3). The human-WG-6 version 3.0 BeadChip (Illumina), which has 48,803 probes, was used for hybridization. The signals for 192 probes (corresponding to 181 genes) were decreased more than 2-fold by Snail expression (supplemental Table 1), whereas the signals for 63 probes (corresponding to 55 genes) were increased more than 2-fold (supplemental Table 2). The list of down-regulated genes includes the E-cadherin gene, which is a well known target of Snail. In addition, some genes related to cell junctions were down-regulated (Table 1). Claudin-3, -7, and -8 are components of tight junctions. These data indicate that EMT was largely regulated at the mRNA level. Genes associated with protein trafficking and degradation were also affected by Snail expression (Table 2). Caveolin-1 and cathepsin L1, which have functions in the endocytosis pathway (45, 46), were up-regulated. Cathepsin L1 is a cysteine proteinase for protein degradation in the lysosome, and cystatin E/M, an inhibitor of cysteine proteinases including cathepsin L1 (47), was down-regulated. In addition, some down-regulated genes were associated with vesicular transport, especially the endosomal recycling pathway (Table 2). Rab proteins are monomeric small GTPases that regulate transport between organelles (48). The Rab family contains more than 60 members in humans. The list of down-regulated genes includes five Rab-associated genes, four of which encode the proteins located in the recycling endosome (*RAB17*, *RAB25*, *RAB40C*, and *RAB11FIP1*) (49–53). Furthermore, *MAL2* is associated with apical sorting in polarized cells (54), and other down-regulated genes involved in the protein transport are shown in Table 2. These data suggest that Snail not only represses target genes related to cell junctions but also influences the expression of genes involved in protein metabolism and distribution, thereby regulating EMT in II-18 cells.

Loss of MV Infection of EMT-induced Polarized Epithelial Cells—We then examined whether MV infection via the epithelial cell receptor is affected by EMT. In these experiments, not only IC323-EGFP or -Luci but also IC/EdH-EGFP or -Luci were used to infect cells. The latter viruses have the H protein of the Edmonston vaccine strain, which can use CD46 as a receptor in addition to SLAM and the epithelial cell receptor. Control and EMT-induced II-18 cells were infected with IC323-EGFP and observed under a fluorescence microscope (Fig. 3*A*). IC323-EGFP infected control cells efficiently and induced cell-cell fusion. By contrast, the number of EGFP-expressing cells was decreased, and syncytium formation was not observed in EMT-induced II-18 cells. CD46-using IC/EdH-EGFP infected both control and EMT-induced cells and induced cell-cell fusion in both (Fig. 3*B*). To quantify the levels of infection, the infectivities of IC323-Luci and IC/EdH-Luci were determined in control and EMT-induced II-18 cells (Fig. 3*C*). IC/EdH-Luci infected both cell types efficiently, and the infectivity was not affected by the induction of EMT. By contrast, the infectivity of IC323-Luci was greatly reduced in EMT-induced II-18 cells compared with control cells. IC/EdH-Luci infected EMT-induced II-18 cells via CD46, because M75, a mAb against CD46, almost completely blocked IC/Ed-H-Luci infection of those cells (Fig. 3*D*). These results clearly indicate that WT MV infection of EMT-induced II-18 cells is abolished at the entry step, very likely due to the absence of a receptor, because CD46-dependent entry and postentry replication of IC/EdH-Luci were not affected at all in EMT-induced II-18 cells. We also performed a fusion assay to obtain additional evidence that MV infection is inhibited at the entry step by the induction of EMT. CHO cells transiently expressing H and F proteins of MV were overlaid onto II-18 cells. CHO cells expressing the H and F proteins can fuse with cells with the corresponding receptors, which can interact with the H protein. Membrane fusion was not observed in EMT-induced II-18 cells when CHO cells expressing the H protein of WT MV were used, but it was observed in those cells when CHO cells expressing the H protein of the MV Edmonston strain were used (Fig. 3*E*). Thus, the H protein of WT MV does not support membrane fusion in EMT-induced II-18 cells, indicating that a receptor for WT MV does not exist in those cells.

We next examined whether EMT also inhibits MV infection in other polarized epithelial cell lines, namely NCI-H358 and HT-29. By expressing Snail, the tight junctions of NCI-H358

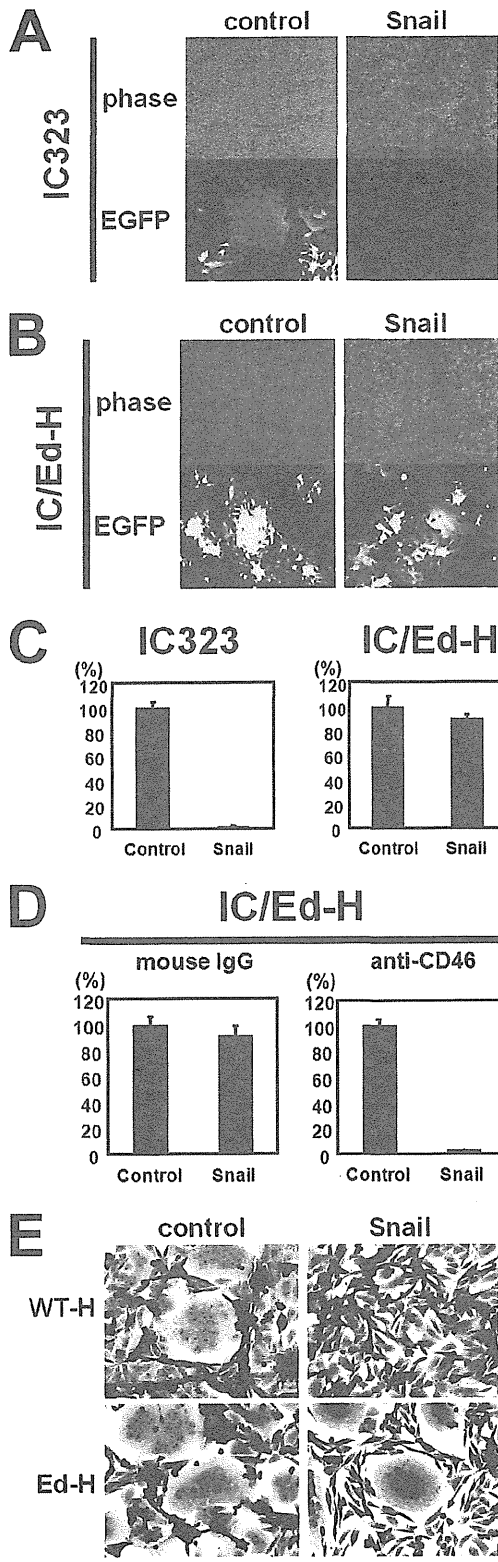

FIGURE 3. **Loss of MV infection of EMT-induced II-18 cells.** *A* and *B*, II-18 cells were infected with the retrovirus vector expressing Snail or control vector at an MOI of 50–100. Control and EMT-induced II-18 cells were infected with IC323-EGFP (*A*) or IC/Ed-H-EGFP (*B*). At 2 days p.i., the cells were observed under a phase-contrast or fluorescence microscope. *C*, control and EMT-induced II-18 cells were infected with IC323-Luci or IC/Ed-H-Luci. At 3 h p.i., the fusion block peptide was added to medium, and at 24 h p.i., the *Renilla* luciferase activity was measured. The activity in control cells was set to 100%. *D*, control and EMT-induced II-18 cells were incubated with medium containing control mouse IgG or a mAb against CD46 (M75) and infected with IC323-Luci. The procedures after MV infection were the same as those in *C*. *E*, CHO cells were transfected with pCA7ps-ICH or pCA7ps-EdH plus pCA7-ICF, using Lipofectamine 2000. Two days after transfection, the cells were harvested and cocultured with II-18 cells. After 2 days of incubation, the cells were subjected to Giemsa staining and observed under a light microscope. *Error bars*, S.D.

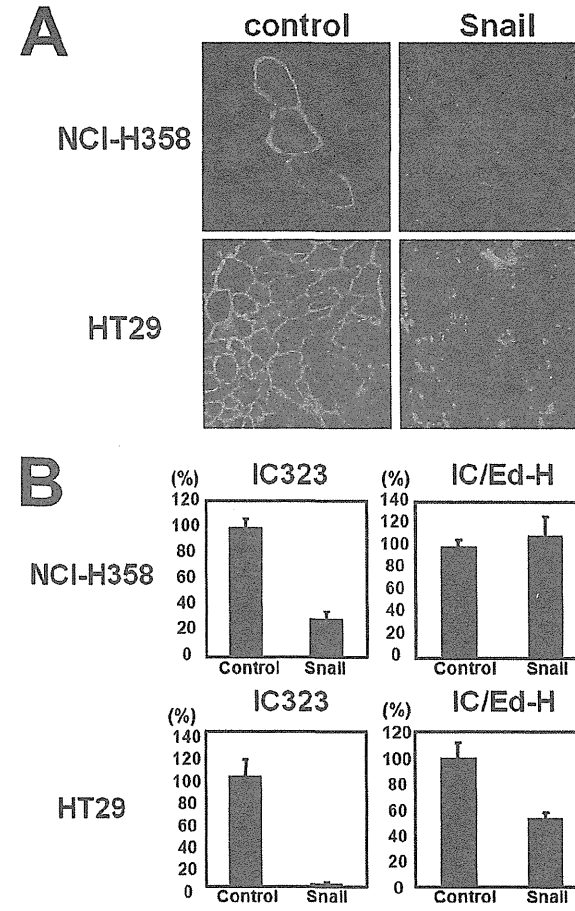

FIGURE 4. **Loss of MV infection of EMT-induced NCI-H358 and HT-29 cells.** *A*, NCI-H358 and HT-29 cells were infected with the retrovirus vector expressing Snail or control vector. At 7–10 days p.i., control and Snail-expressing cells were permeabilized, fixed, and stained with a mAb against ZO-1, followed by incubation with Alexa Fluor 488-conjugated anti-mouse secondary antibody. Nuclear DNA was stained with propidium iodide. The cells were observed using a confocal microscope. *B*, control and Snail-expressing cells were infected with IC323-Luci or IC/Ed-H-Luci. At 3 h p.i., the fusion block peptide was added to medium, and at 24 h p.i., the *Renilla* luciferase activity was measured. The activity in control cells was set to 100%. *Error bars*, S.D.

and HT-29 cells were destroyed, as revealed by staining for ZO-1 (Fig. 4*A*). At 5 days after the induction of EMT with the retrovirus vector encoding Snail, NCI-H358 and HT-29 cells were infected with 1.0×10^3 plaque-forming units of IC323-Luci or IC323/Ed-H-Luci. The infectivity of IC323-Luci, but not IC/Ed-H-Luci, was reduced in EMT-induced NCI-H358 cells (Fig. 4*B*). The infectivity of IC323-Luci was almost completely abolished in EMT-induced HT-29 cells, whereas that of IC/Ed-H-Luci was only moderately reduced (Fig. 4*B*). Thus, the induction of EMT in polarized epithelial cells is correlated with the loss of infectivity of WT MV. These results indicate that the

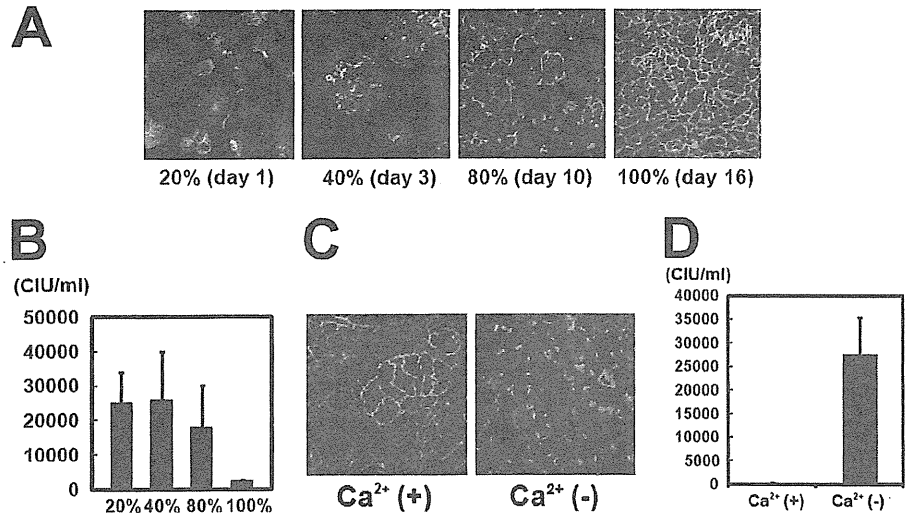

FIGURE 5. **WT MV infection of HT-29 cells with or without tight junctions.** *A*, HT-29 cells were seeded on culture plates to fill ~15% of the culture area. At day 1, 3, 10, and 16 (when growing cells filled 20, 40, 80, and 100% of the culture area, respectively), cells were permeabilized, fixed, and stained with a mAb against ZO-1, followed by incubation with Alexa Fluor 488-conjugated anti-mouse secondary antibody. Nuclear DNA was stained with propidium iodide. The cells were observed using a confocal microscope. *B*, HT-29 cells grown under the same conditions as those in *A* were infected with 2.0×10^5 CIU of IC323-EGFP for 2 h (CIUs were determined on Vero/hSLAM cells). After 2 h of incubation, cells were washed with PBS and incubated in a standard culture medium with the fusion block peptide. Numbers of EGFP-expressing cells were counted at 2 days p.i. *C*, at 8–12 days after plating, HT-29 cells were fed with Ca^{2+}-free medium or medium containing Ca^{2+}. After 24 h of incubation, cells were used for immunostaining as in *A*. *D*, HT-29 cells grown under the same conditions as those in *C* were infected with IC323-EGFP, and CIUs were determined at 2 days p.i. *Error bars*, S.D.

putative MV receptor on polarized epithelial cells disappears upon the induction of EMT.

The Formation of Junction Structures per Se Is Not Required for WT MV Infection—Last, experiments were performed to investigate whether the formation of junction structures, such as tight and adherens junctions, is necessary for MV to enter polarized epithelial cells. Polarized cells form tight junctions when growing densely in monolayers (55). HT-29 cells have the ability to form complete monolayers with the formation of tight junctions and can be propagated uniformly (Fig. 4A), unlike most other human polarized epithelial cell lines. HT-29 cells were seeded on culture plates to fill ~15% of the culture area (day 0). On days 1 and 3, HT-29 cells filled ~20 and ~40% of the culture area, respectively, and poorly formed tight junctions (Fig. 5*A*). When the cells filled ~80% of the culture area, on day 10, about half of the cells formed tight junctions (Fig. 5*A*). On day 16, cells filled the culture area almost entirely (100%), forming tight junctions well (Fig. 5*A*). These monolayers cultured in different densities were infected with 2.0×10^5 CIU of IC323-EGFP. To determine the initial infection of these monolayers by IC323-EGFP, the second round of infection was blocked by a fusion block peptide (34, 43). When the numbers of EGFP-expressing cells were counted at 2 days p.i., they were 2.5×10^4, 2.6×10^4, 1.8×10^4, and 2.3×10^3 in monolayers at densities of ~20, 40, 80, and 100%, respectively (Fig. 5*B*). These data indicate that, when cells form tight junctions completely, the infection efficiency of WT MV becomes lower compared with that in cells having incomplete tight junctions.

We also analyzed the role of junction structure formation in WT MV infection in a different way. Ca^{2+} is a critical component for the formation of tight junctions (55). When Ca^{2+} is depleted from culture media, cells no longer form tight junctions (55). Confluent monolayers of HT-29 cells forming tight junctions were prepared. Before infection with MV, some monolayers were cultured in DMEM containing Ca^{2+} and others in Ca^{2+}-free medium. After 24 h of incubation, the latter lost tight junctions (Fig. 5*C*), as reported previously (55). These monolayers with or without tight junctions were infected with 1×10^5 CIU of IC323-EGFP and cultured in the presence of the fusion block peptide. When counted at 2 days p.i., the number of EGFP-expressing cells was more than 100 times greater in monolayers without tight junctions than in those retaining the junctions (Fig. 5*D*). These data indicate that the formation of tight junctions *per se* is not required for WT MV infection and rather restricts MV infection.

DISCUSSION

MV predominantly infects immune cells *in vivo* by using SLAM as a receptor (56, 57), explaining the lymphotropism and immunosuppressive nature of MV. However, MV also infects polarized epithelial cells independently of SLAM (14–16). The ability of MV to infect polarized epithelial cells may not be required to cause disease symptoms but appears to be important for its transmission (16). Thus, the unknown epithelial cell receptor should be identified and investigated to fully understand MV pathogenesis. In this study, we have shown that the induction of EMT almost completely abolishes the susceptibility of polarized epithelial cell lines to WT MV, shedding light on the properties of the epithelial cell receptor.

We found that a lung adenocarcinoma cell line II-18 is very useful to study the mechanisms underlying MV infection of epithelial cells. II-18 cells are easily cultured in a standard culture medium, unlike other human polarized epithelial cell lines, and are highly susceptible to WT MV independently of SLAM and CD46. Furthermore, they are readily induced to undergo EMT by expressing the transcriptional repressor Snail in them. Upon expression of Snail, II-18 cells lost intercellular adherens and tight junctions, accompanied by the up- and down-regulation of a number of genes, as revealed by microarray analysis.

Previous studies reported that Snail affects gene expression of molecules involved in the cell junctions, cytoskeleton, cell metabolism, transcription, and cell signaling (26, 58, 59). Our results showed that Snail also affects the expression of genes

responsible for protein degradation and trafficking. The list of up-regulated genes included those encoding caveolin-1 and cathepsin L1, which function in the endocytosis pathway (45, 46). By contrast, the gene encoding cystatin E/M, an inhibitor of cysteine proteinases, such as cathepsin L1 (47), was down-regulated. Furthermore, the list of down-regulated genes contained those encoding proteins involved in protein trafficking, especially protein recycling. De Craene *et al.* (26) also reported that RAB25 is repressed by Snail. Endocytosed proteins escape from degradation in the lysosome if they are transported to the recycling endosome and returned to the plasma membrane (60). The recycling endosome is also associated with apical/basolateral sorting, which maintains the polarity of the cell membrane (60). Thus, it is likely that Snail inhibits the recycling pathway and enhances protein degradation, thereby affecting the distribution of proteins. Together with down-regulation of genes encoding cell junction molecules, this may contribute to Snail-mediated EMT in II-18 cells. Similar observations have been reported. E-cadherin was found to be endocytosed and degraded in lysosomes when EMT was induced by TGF-β (61). Ohkubo *et al.* (22) showed that the tight junction constituent claudin-1 is down-regulated by Snail expression at the post-transcriptional level, although another group reported a different observation (23).

All cell lines that WT MV has been shown to infect in a SLAM-independent manner are polarized epithelial cells forming tight junctions. Therefore, we thought that EMT might affect the susceptibility of II-18 cells to MV. Beyond our initial expectations, EMT almost completely abolished MV infection of II-18 cells via the epithelial cell receptor. Inhibition of MV infection was at the entry step, because entry and membrane fusion mediated by CD46-using MV were not affected by EMT. The same findings were obtained in other polarized cell lines, namely NCI-H358 and HT-29. These data indicate that the unidentified epithelial cell receptor for MV is a polarized epithelial cell-specific molecule that disappears from the plasma membrane of II-18 cells upon the induction of EMT. It is also reported that EMT inhibits adenovirus infection through down-regulation of the coxsackie and adenovirus receptor (62), which is a component of the tight junction (63).

Despite the above findings, the formation of junction structures was not required for MV to enter polarized epithelial cells. On the contrary, the complete formation of tight junctions restricted MV entry into HT-29 cells. This indicates that the access of MV to the epithelial cell receptor is hindered when junction structures are completely formed. Infection by hepatitis C virus, which utilizes the tight junction molecules claudin and occludin as receptors, is reported to be restricted by cell polarization (64). The epithelial cell receptor for MV may also be a component of tight or adherens junctions. Alternatively, it may be a molecule strictly present at the basolateral surface of epithelial cells.

In an attempt to identify the putative epithelial cell receptor for MV, we knocked down, by using small interfering RNA, the molecules whose expressions are down-regulated by induced EMT. Although we have thus far tried small interfering RNAs for more than a dozen molecules, including *CD9*, *CDH1*, *CLDN3*, *CLDN7*, *MAL2*, *MALL*, and *STX3* (Tables 1 and 2), the infectivity of MV is not affected in treated cells.

Identification of the epithelial cell receptor for MV will contribute to better understanding of MV pathogenesis, because the use of the epithelial cell receptor is important for MV transmission (15, 16). Thus, we continue to make efforts to identify this receptor. Furthermore, the present study suggests that susceptibility to MV may be used to monitor EMT or mesenchymal-epithelial transition (65).

Acknowledgments—We thank Y. Fujinaga for HT-29 cells; T. Seya for M75 hybridoma cells; M. Shimojima and T. Kitamura for PLAT-gp cells, pMX, pMX-GFP, pMXs-IP, and pCVSV-G; M. A. Billter for Edmonston tag cDNA; and K. Takayama for various human cell lines. We also thank the staff of the Research Support Center (Faculty of Medicine, Kyushu University) for technical support of microarray analysis.

REFERENCES

1. Bryce, J., Boschi-Pinto, C., Shibuya, K., and Black, R. E. (2005) *Lancet* **365,** 1147–1152
2. Tatsuo, H., Ono, N., Tanaka, K., and Yanagi, Y. (2000) *Nature* **406,** 893–897
3. Dörig, R. E., Marcil, A., Chopra, A., and Richardson, C. D. (1993) *Cell* **75,** 295–305
4. Naniche, D., Varior-Krishnan, G., Cervoni, F., Wild, T. F., Rossi, B., Rabourdin-Combe, C., and Gerlier, D. (1993) *J. Virol.* **67,** 6025–6032
5. Craighead, J. E. (2000) in *Pathology and Pathogenesis of Human Viral Disease* (Craighead, J. E., ed) pp. 397–410, Elsevier, London, UK
6. Kimura, A., Tosaka, K., and Nakao, T. (1975) *Arch. Virol.* **47,** 295–307
7. Lightwood, R., and Nolan, R. (1970) *J. Pediatr.* **77,** 59–64
8. Moench, T. R., Griffin, D. E., Obriecht, C. R., Vaisberg, A. J., and Johnson, R. T. (1988) *J. Infect. Dis.* **158,** 433–442
9. Nii, S., Kamahora, J., Mori, Y., Takahashi, M., Nishimura, S., and Okuno, Y. (1964) *Biken J.* **6,** 271–297
10. Nommensen, F. E., and Dekkers, N. W. (1981) *J. Med. Virol.* **7,** 157–162
11. Olding-Stenkvist, E., and Bjorvatn, B. (1976) *J. Infect. Dis.* **134,** 463–469
12. Sakaguchi, M., Yoshikawa, Y., Yamanouchi, K., Sata, T., Nagashima, K., and Takeda, K. (1986) *Microbiol. Immunol.* **30,** 1067–1073
13. Takeuchi, K., Miyajima, N., Nagata, N., Takeda, M., and Tashiro, M. (2003) *Virus Res.* **94,** 11–16
14. Takeda, M., Tahara, M., Hashiguchi, T., Sato, T. A., Jinnouchi, F., Ueki, S., Ohno, S., and Yanagi, Y. (2007) *J. Virol.* **81,** 12091–12096
15. Tahara, M., Takeda, M., Shirogane, Y., Hashiguchi, T., Ohno, S., and Yanagi, Y. (2008) *J. Virol.* **82,** 4630–4637
16. Leonard, V. H., Sinn, P. L., Hodge, G., Miest, T., Devaux, P., Oezguen, N., Braun, W., McCray, P. B., Jr., McChesney, M. B., and Cattaneo, R. (2008) *J. Clin. Invest.* **118,** 2448–2458
17. Thiery, J. P., and Sleeman, J. P. (2006) *Nat. Rev. Mol. Cell Biol.* **7,** 131–142
18. Barrallo-Gimeno, A., and Nieto, M. A. (2005) *Development* **132,** 3151–3161
19. Batlle, E., Sancho, E., Francí, C., Domínguez, D., Monfar, M., Baulida, J., and García De Herreros, A. (2000) *Nat. Cell Biol.* **2,** 84–89
20. Cano, A., Pérez-Moreno, M. A., Rodrigo, I., Locascio, A., Blanco, M. J., del Barrio, M. G., Portillo, F., and Nieto, M. A. (2000) *Nat. Cell Biol.* **2,** 76–83
21. Ikenouchi, J., Matsuda, M., Furuse, M., and Tsukita, S. (2003) *J. Cell Sci.* **116,** 1959–1967
22. Ohkubo, T., and Ozawa, M. (2004) *J. Cell Sci.* **117,** 1675–1685
23. Martínez-Estrada, O. M., Cullerés, A., Soriano, F. X., Peinado, H., Bolós, V., Martínez, F. O., Reina, M., Cano, A., Fabre, M., and Vilaró, S. (2006) *Biochem. J.* **394,** 449–457
24. Whiteman, E. L., Liu, C. J., Fearon, E. R., and Margolis, B. (2008) *Oncogene* **27,** 3875–3879
25. Guaita, S., Puig, I., Franci, C., Garrido, M., Dominguez, D., Batlle, E., San-

cho, E., Dedhar, S., De Herreros, A. G., and Baulida, J. (2002) *J. Biol. Chem.* **277,** 39209–39216
26. De Craene, B., Gilbert, B., Stove, C., Bruyneel, E., van Roy, F., and Berx, G. (2005) *Cancer Res.* **65,** 6237–6244
27. Kobayashi, S., Okada, S., Inaba, H., Syoji, W., Hasumi, T., Sato, N., and Fujimura, S. (1990) *Kokenshi* **42,** 73–79
28. Morita, S., Kojima, T., and Kitamura, T. (2000) *Gene Ther.* **7,** 1063–1066
29. Ono, N., Tatsuo, H., Hidaka, Y., Aoki, T., Minagawa, H., and Yanagi, Y. (2001) *J. Virol.* **75,** 4399–4401
30. Brower, M., Carney, D. N., Oie, H. K., Gazdar, A. F., and Minna, J. D. (1986) *Cancer Res.* **46,** 798–806
31. Fogh, J., and G. Trempe. (1975) in *Human Tumor Cells in Vitro* (Fogh, J., ed) pp. 115–160, Plenum Publishing Corp., New York
32. Giard, D. J., Aaronson, S. A., Todaro, G. J., Arnstein, P., Kersey, J. H., Dosik, H., and Parks, W. P. (1973) *J. Natl. Cancer Inst.* **51,** 1417–1423
33. Takeda, M., Takeuchi, K., Miyajima, N., Kobune, F., Ami, Y., Nagata, N., Suzaki, Y., Nagai, Y., and Tashiro, M. (2000) *J. Virol.* **74,** 6643–6647
34. Hashimoto, K., Ono, N., Tatsuo, H., Minagawa, H., Takeda, M., Takeuchi, K., and Yanagi, Y. (2002) *J. Virol.* **76,** 6743–6749
35. Tahara, M., Takeda, M., Seki, F., Hashiguchi, T., and Yanagi, Y. (2007) *J. Virol.* **81,** 2564–2572
36. Takeda, M., Ohno, S., Seki, F., Hashimoto, K., Miyajima, N., Takeuchi, K., and Yanagi, Y. (2005) *Virus Res.* **108,** 161–165
37. Nakatsu, Y., Takeda, M., Kidokoro, M., Kohara, M., and Yanagi, Y. (2006) *J. Virol. Methods* **137,** 152–155
38. Niwa, H., Yamamura, K., and Miyazaki, J. (1991) *Gene* **108,** 193–199
39. Kitamura, T., and Morikawa, Y. (2000) *Methods Mol. Biol.* **134,** 143–152
40. Onishi, M., Kinoshita, S., Morikawa, Y., Shibuya, A., Phillips, J., Lanier, L. L., Gorman, D. M., Nolan, G. P., Miyajima, A., and Kitamura, T. (1996) *Exp. Hematol.* **24,** 324–329
41. Kitamura, T., Koshino, Y., Shibata, F., Oki, T., Nakajima, H., Nosaka, T., and Kumagai, H. (2003) *Exp. Hematol.* **31,** 1007–1014
42. Takeda, M., Ohno, S., Seki, F., Nakatsu, Y., Tahara, M., and Yanagi, Y. (2005) *J. Virol.* **79,** 14346–14354
43. Richardson, C. D., Scheid, A., and Choppin, P. W. (1980) *Virology* **105,** 205–222
44. Sidorenko, S. P., and Clark, E. A. (1993) *J. Immunol.* **151,** 4614–4624
45. Mayor, S., and Pagano, R. E. (2007) *Nat. Rev. Mol. Cell Biol.* **8,** 603–612
46. Turk, V., Turk, B., and Turk, D. (2001) *EMBO J.* **20,** 4629–4633
47. Cheng, T., Hitomi, K., van Vlijmen-Willems, I. M., de Jongh, G. J., Yamamoto, K., Nishi, K., Watts, C., Reinheckel, T., Schalkwijk, J., and Zeeuwen, P. L. (2006) *J. Biol. Chem.* **281,** 15893–15899
48. Zerial, M., and McBride, H. (2001) *Nat. Rev. Mol. Cell Biol.* **2,** 107–117
49. Hunziker, W., and Peters, P. J. (1998) *J. Biol. Chem.* **273,** 15734–15741
50. Zacchi, P., Stenmark, H., Parton, R. G., Orioli, D., Lim, F., Giner, A., Mellman, I., Zerial, M., and Murphy, C. (1998) *J. Cell Biol.* **140,** 1039–1053
51. Casanova, J. E., Wang, X., Kumar, R., Bhartur, S. G., Navarre, J., Woodrum, J. E., Altschuler, Y., Ray, G. S., and Goldenring, J. R. (1999) *Mol. Biol. Cell* **10,** 47–61
52. Rodriguez-Gabin, A. G., Almazan, G., and Larocca, J. N. (2004) *J. Neurosci. Res.* **76,** 758–770
53. Hales, C. M., Griner, R., Hobdy-Henderson, K. C., Dorn, M. C., Hardy, D., Kumar, R., Navarre, J., Chan, E. K., Lapierre, L. A., and Goldenring, J. R. (2001) *J. Biol. Chem.* **276,** 39067–39075
54. de Marco, M. C., Martín-Belmonte, F., Kremer, L., Albar, J. P., Correas, I., Vaerman, J. P., Marazuela, M., Byrne, J. A., and Alonso, M. A. (2002) *J. Cell Biol.* **159,** 37–44
55. Siliciano, J. D., and Goodenough, D. A. (1988) *J. Cell Biol.* **107,** 2389–2399
56. de Swart, R. L., Ludlow, M., de Witte, L., Yanagi, Y., van Amerongen, G., McQuaid, S., Yüksel, S., Geijtenbeek, T. B., Duprex, W. P., and Osterhaus, A. D. (2007) *PLoS Pathog.* **3,** e178
57. Yanagi, Y., Takeda, M., Ohno, S., and Hashiguchi, T. (2009) *Curr. Top. Microbiol. Immunol.* **329,** 13–30
58. Moreno-Bueno, G., Cubillo, E., Sarrió, D., Peinado, H., Rodríguez-Pinilla, S. M., Villa, S., Bolós, V., Jordá, M., Fabra, A., Portillo, F., Palacios, J., and Cano, A. (2006) *Cancer Res.* **66,** 9543–9556
59. Vetter, G., Le Béchec, A., Muller, J., Muller, A., Moes, M., Yatskou, M., Al Tanoury, Z., Poch, O., Vallar, L., and Friederich, E. (2009) *Biochem. Biophys. Res. Commun.* **385,** 485–491
60. Grant, B. D., and Donaldson, J. G. (2009) *Nat. Rev. Mol. Cell Biol.* **10,** 597–608
61. Janda, E., Nevolo, M., Lehmann, K., Downward, J., Beug, H., and Grieco, M. (2006) *Oncogene* **25,** 7117–7130
62. Lacher, M. D., Tiirikainen, M. I., Saunier, E. F., Christian, C., Anders, M., Oft, M., Balmain, A., Akhurst, R. J., and Korn, W. M. (2006) *Cancer Res.* **66,** 1648–1657
63. Cohen, C. J., Shieh, J. T., Pickles, R. J., Okegawa, T., Hsieh, J. T., and Bergelson, J. M. (2001) *Proc. Natl. Acad. Sci. U.S.A.* **98,** 15191–15196
64. Mee, C. J., Grove, J., Harris, H. J., Hu, K., Balfe, P., and McKeating, J. A. (2008) *J. Virol.* **82,** 461–470
65. Saito, R. A., Watabe, T., Horiguchi, K., Kohyama, T., Saitoh, M., Nagase, T., and Miyazono, K. (2009) *Cancer Res.* **69,** 2783–2791

JOURNAL OF VIROLOGY, Nov. 2010, p. 11189–11199 Vol. 84, No. 21
0022-538X/10/$12.00 doi:10.1128/JVI.01075-10

The F Gene of the Osaka-2 Strain of Measles Virus Derived from a Case of Subacute Sclerosing Panencephalitis Is a Major Determinant of Neurovirulence▽

Minoru Ayata,[1]* Kaoru Takeuchi,[2] Makoto Takeda,[3] Shinji Ohgimoto,[1] Seiichi Kato,[1] Luna Bhatta Sharma,[1] Miyuu Tanaka,[4] Mitsuru Kuwamura,[4] Hiroshi Ishida,[1,5] and Hisashi Ogura[1]

Department of Virology, Osaka City University Medical School, Osaka 545-8585, Japan[1]; Department of Infection Biology, Graduate School of Comprehensive Human Sciences and Institute of Basic Medical Sciences, University of Tsukuba, Ibaraki 305-8575, Japan[2]; Department of Virology III, National Institute of Infectious Diseases, Tokyo 208-0011, Japan[3]; Laboratory of Veterinary Pathology, Osaka Prefecture University, Osaka 598-8531, Japan[4]; and Department of Pediatrics, Izumi Municipal Hospital, Osaka 594-0071, Japan[5]

Received 19 May 2010/Accepted 11 August 2010

Measles virus (MV) is the causative agent for acute measles and subacute sclerosing panencephalitis (SSPE). Although numerous mutations have been found in the MV genome of SSPE strains, the mutations responsible for the neurovirulence have not been determined. We previously reported that the SSPE Osaka-2 strain but not the wild-type strains of MV induced acute encephalopathy when they were inoculated intracerebrally into 3-week-old hamsters. The recombinant MV system was adapted for the current study to identify the gene(s) responsible for neurovirulence in our hamster model. Recombinant viruses that contained envelope-associated genes from the Osaka-2 strain were generated on the IC323 wild-type MV background. The recombinant virus containing the M gene alone did not induce neurological disease, whereas the H gene partially contributed to neurovirulence. In sharp contrast, the recombinant virus containing the F gene alone induced lethal encephalopathy. This phenotype was related to the ability of the F protein to induce syncytium formation in Vero cells. Further study indicated that a single T461I substitution in the F protein was sufficient to transform the nonneuropathogenic wild-type MV into a lethal virus for hamsters.

Measles virus (MV) is a member of the *Morbillivirus* genus in the *Paramyxoviridae* family, and its genome is a nonsegmented single-stranded RNA of negative polarity. The MV genome contains N, P, M, F, H, and L genes. The genome is covered with the nucleocapsid (N) protein, which is transcribed from the N gene. The P gene encodes the phospho-protein (P), which forms the replicase complex with the large (L) polymerase protein encoded by the L gene. In addition to encoding the P protein, the P gene encodes accessory C and V proteins, which counteract antiviral host defense. The envelope of the virion consists of the two transmembrane glycoproteins, fusion (F) and hemagglutinin (H), which are transcribed from the F and H genes, respectively. The M gene encodes the matrix (M) protein, which associates with nucleocapsids and with the cytoplasmic regions of the F and H proteins (25). The signaling lymphocyte activation molecule (SLAM, also designated CD150) is the primary receptor for wild-type MV (22, 27, 69), and specific amino acid changes (N481Y or S546G) in the MV H protein present in some MV strains are required for interaction between the H protein and CD46 (23, 26, 39, 42, 46, 56, 62).

MV is the causative agent of measles and, on very rare occasions, causes subacute sclerosing panencephalitis (SSPE). SSPE is a fatal degenerative disease caused by persistent MV infection of the central nervous system (59). On rare occasions, MV has been isolated from brain cells of patients with SSPE by cocultivation with cell lines susceptible to MV (48). Genetic analyses revealed that these viruses derived from SSPE patients (SSPE strains) contain numerous mutations, and the existence of characteristic or frequently found mutations common to SSPE strains was suggested (3, 14). The M gene of SSPE strains seems particularly vulnerable to mutation, and its expression is restricted. In many SSPE strains, an A-to-G-biased hypermutation occurred in the genome and destroyed the M protein-coding frames. In some cases, translation of the M protein is complicated by a transcriptional defect that leads to an almost exclusive synthesis of dicistronic P-M mRNA (4, 12, 13, 61). Elucidation of the mechanism of the aberrant read-through transcription at the P-M gene junction revealed that a single deletion or mutation at the P gene end was responsible (5). Another characteristic change of the structural protein found in SSPE strains is located in the F protein (8, 16, 47, 57). A mutation in the termination codon of the F protein in some strains resulted in an elongated cytoplasmic domain. Another type of mutation created a premature termination codon in the F protein-coding frame and resulted in a shortened cytoplasmic domain. In some strains, including the SSPE Osaka-2 strain, one mutation did not change the length of the cytoplasmic domain, but multiple mutations in the reading frame caused nonconservative amino acid substitutions. Some

* Corresponding author. Mailing address: Department of Virology, Osaka City University Medical School, 1-4-3 Asahimachi, Abeno-ku, Osaka 545-8585, Japan. Phone: 81 6 6645 3911. Fax: 81 6 6645 3912. E-mail: maverick@med.osaka-cu.ac.jp.

▽ Published ahead of print on 18 August 2010.

of the mutations developed in this domain can be explained by the biased hypermutation that is more frequently and extensively found in the M gene, as mentioned above (15, 16). However, the effects of these hypermutations as well as of other sporadic mutations in the genome of SSPE strains have been poorly understood.

The ability to induce syncytia in Vero cells is one of the characteristic features of SSPE strains *in vitro*. Triggered by the binding of the H protein to the cellular receptor, the F protein plays a central role in virus-cell and cell-to-cell fusion. We previously demonstrated that the F protein of three SSPE strains (Osaka-1, Osaka-2, and Osaka-3 strains) induced syncytia in Vero cells when coexpressed with the H protein from any MV strain, including the wild-type MVs (6). In addition, the region responsible for the enhanced fusion was further narrowed to the extracellular domain of the F protein. Whether the enhanced fusion activity is related to the neurovirulence is still unclear.

MVs generally do not induce neurological disease in experimental small animals. Brain-adapted strains can replicate in newborn animals, but neurovirulence is reduced as the animal ages (1, 7, 9, 24). Transgenic mice expressing human CD46 or SLAM were established and observed for MV infection (19, 37, 45, 50, 52, 60). In a transgenic line which expresses SLAM ubiquitously (60), infection of the central nervous system was examined, and this revealed that MV could induce an acute neurological syndrome in mice less than 3 weeks old. In contrast, SSPE strains show strong neurovirulence and can induce lethal neurological disease in immunocompetent, genetically unaltered animals (2, 31, 32, 33, 64, 70). We previously reported that the SSPE Osaka-2 strain induced acute encephalopathy in 3-week-old hamsters several days after intracerebral inoculation (29). Therefore, it is important to analyze the differential roles of the mutations found in the genome of SSPE strains to understand the molecular mechanism of MV persistence in the brain and the pathogenesis of SSPE. Cathomen et al. described the role of mutations found in SSPE strains by adapting the recombinant MV system (10). In a similar system, Patterson et al. also described the role of the mutation in the M gene (52). These results indicated that expression of the defective M protein or defects in the cytoplasmic tail of the envelope glycoproteins resulted in the attenuation of MV neurovirulence in mice, but enhancing factors responsible for MV neurovirulence have not been determined. Because genetically unaltered young adult hamsters are highly susceptible to infection with SSPE strains, show clear symptoms, and tolerate infection for 2 or 3 days and because, practically, a higher titer of virus stock can be inoculated into brain, we have been using hamsters for the analyses of MV neurovirulence. The recombinant MV system (53, 58, 65) was adapted for the current study to identify the gene(s) responsible for neurovirulence in our hamster model.

We found that mutations in the F and H protein-coding genes of the SSPE Osaka-2 strain were responsible for neurovirulence. Further investigation demonstrated that a single amino acid substitution in the F protein transformed the nonneuropathogenic wild-type MV IC323 strain into a lethal virus similar to the SSPE Osaka-2 strain in hamsters.

MATERIALS AND METHODS

Cells and viruses. CHO cells expressing CD46 (CHO/CD46) cells (a gift of Y. Murakami, Department of Pharmaceutical Sciences, Hokkaido University) (30) were cultured in RPMI 1640 medium (Nissui Pharmaceutical Co., Tokyo, Japan) supplemented with 5% heat-inactivated fetal calf serum (FCS) and 0.7 mg of hygromycin (Nacalai Tesque, Tokyo, Japan) per ml. CHO/SLAM and Vero/SLAM cells (gifts of Y. Yanagi, Department of Virology, Graduate School of Medical Sciences, Kyushu University) (51, 69) were cultured in Dulbecco's modified Eagle's medium (DMEM; Nissui Pharmaceutical) supplemented with 10% FCS and 0.5 mg of G418 (Nacalai Tesque) per ml. B95a cells (34) were grown in RPMI 1640 medium supplemented with 10% FCS. Vero, 293T, CHO, IMR-32, SK-N-SH, A172, and U-251 cells (63) were cultured in DMEM supplemented with 10% FCS.

Isolation of sibling viruses (Osaka-2/FrV and Osaka-2/FrB) of the SSPE Osaka-2 strain was described previously (48). These sibling viruses were neurovirulent when they were injected into hamster brains (29).

Plasmids. Plasmids were cloned in the mammalian expression vector pME18S, which contained genes encoding the entire F or H protein region, as described previously (6). Plasmids encoding chimeric F proteins, OSA2-ext and OSA2-cyt, were previously described as Osa2/Toy and Mas/Osa2, respectively (6). The nucleotide sequences of the M, F, and H genes of the Osaka-2 strain were reported previously (4, 23, 47). Plasmids encoding mutant F proteins were constructed by a PCR-based method with synthetic primer pairs, and the inserts were confirmed by sequencing. Plasmids encoding the mutant MV genome were based on p(+)MV323, which encodes the antigenomic full-length cDNA of the wild-type IC-B strain (65). For construction of plasmids to prepare recombinant viruses containing the M gene, SalI and BstEII sites located in the 3′ noncoding regions of the P and M genes, respectively, were used for cloning. Because the BstEII site is found in the coding region but not in the 3′ noncoding region of the M gene of the Osaka-2 strain, synthetic primers were used to destroy the BstEII site in the coding region (5′-^{3997}CCTTCAACCTGCTAGTGACC^{4016}-3′ and 5′-^{4016}GGTCACTAGCAGGTTGAAGG^{3997}-3′) and to create a BstEII site in the 3′ noncoding region (5′-^{4820}GCGGTTGGGTCACCTCGACCGC^{4799}-3′). To construct plasmids for preparation of recombinant viruses containing the F and H genes, BsmBI and SpeI sites and SpeI and PacI sites were used for cloning, respectively.

Transient expression of F and H glycoproteins and indirect immunofluorescence microscopy. Cells grown on Sonic seal slide wells (Nalge Nunc International, Rochester, NY) were transfected with 0.5 μg of F-containing plasmids and 0.5 μg of H-containing plasmids per well using Lipofectamine LTX transfection reagent (Invitrogen, Carlsbad, CA) according to the manufacturer's protocol.

Transfected cells were incubated at 35°C for 24 h. The cells were washed once with phosphate-buffered saline (pH 7.4), air dried, and fixed with a 1:1 acetone-methanol mixture at room temperature for 2 min. Monoclonal antibody to the H protein was used for the immunofluorescent staining as described previously (6).

Preparation of recombinant MV that expresses proteins derived from SSPE. Recombinant MVs were generated from cDNAs by using CHO/SLAM cells and the vaccinia virus carrying T7 RNA polymerase, vTF7-3, according to a previously described procedure (66). To obtain cell-free virus stock, infected B95a cells were treated with cytochalasin D (CD; Sigma, St. Louis, MO) as previously described (28), and the resulting virus-like particles (CD-VLP) were stored at −85°C. Infectivity titers of the virus stock were determined by determining the number of PFU in B95a cells or in other cell lines such as Vero or Vero/SLAM cells.

Virus inoculation into and recovery from hamsters and histopathological examination. Three-week-old female Syrian golden hamsters (SLC-Japan, Shizuoka, Japan) were gently anesthetized with ether, and 50 μl of properly diluted CD-VLP stock was inoculated into the right hemisphere of the brain. Selected hamsters from each group were sacrificed, and the brains were removed and subjected to either virus rescue or histopathological examination. Virus was recovered from brain cells by cocultivation with B95a cells. Total cellular RNA was extracted from the recovered virus-infected cells or directly from the brain according to a previously described method (4). The RNA was reverse transcribed, and the regions containing the M, F, or H gene were amplified by PCR and sequenced. Removed whole brains were fixed with 10% formalin (Wako Pure Chemicals, Osaka, Japan). Sections were prepared and stained with hematoxylin and eosin and evaluated histopathologically. All animal experiments were performed according to the Guide for Animal Experimentation, Osaka City University, in the infected-animal room at the biosafety level 2 Laboratory Center of the Medical School.

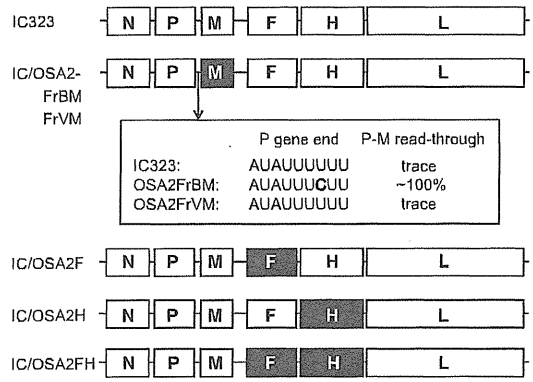

FIG. 1. Schematic diagram of the genome of the recombinant MVs. The protein-coding regions (N, P, M, F, H, and L) of the IC323 strain are shown as open boxes. The M, F, and H protein-coding regions derived from the Osaka-2 strain are shown as filled boxes. The sequence of the P gene end of the two sibling viruses (OSA2FrBM and OSA2FrVM) of the Osaka-2 strain and the extents of the transcriptional read-through at the P-M gene junction are indicated.

RESULTS

The M gene of the SSPE Osaka-2 strain is not a determinant of neurovirulence. Many mutations are found in the MV genome from SSPE strains, and the M gene is the most affected. To test the consequences of M gene mutation on neurovirulence in our hamster model, we generated recombinant viruses in which the M gene of the IC323 strain was replaced with that of the SSPE Osaka-2 strain (Fig. 1). Because the difference in the P gene end sequences of the two sibling viruses (Osaka-2/FrB and Osaka-2/FrV) of the strain (29) affected transcription of the M gene (5), the P gene end region of each sibling virus was included in the constructs. The resulting recombinant IC/OSA2FrBM virus produces almost exclusively dicistronic P-M mRNA, whereas the IC/OSA2FrVM virus produces monocistronic P and M mRNAs.

The recombinant viruses were propagated on B95a cells, and CD-VLP were prepared and stored as described in Materials and Methods. The CD-VLP stock was titrated on B95a cells (Fig. 2A). The titers of the recombinant viruses containing the M gene derived from both sibling viruses were similar when viruses were titrated in B95a cells. The CD-VLP stock was also titrated on Vero/SLAM cells, and the titers were higher than in B95a cells and comparable between the two viruses. In contrast, no detectable cytopathic effects such as syncytium formation were observed in CD-VLP-infected Vero cells.

Infectious cell-free virus production was assayed by B95a cell culture (Fig. 2B and C). Wild-type IC323 virus produced significant amounts of cell-free virus particles, whereas the IC/OSA2FrBM and IC/OSA2FrVM viruses produced minimum amounts of both the extracellular and intracellular cell-free virus particles. This suggested that the defective expression of the Osaka-2 M gene affected virus particle production, probably during the budding process, which was demonstrated by another nonproductive SSPE strain (52).

The recombinant IC/OSA2FrBM and IC/OSA2FrVM viruses were inoculated intracerebrally into 3-week-old hamsters, and neurovirulence was evaluated (Table 1). No hamster developed any neurological signs during the course of observation. In the same manner, no hamster that was inoculated with the IC323 virus (850 PFU/brain or 11,500 PFU/brain) showed any symptoms during the course of observation.

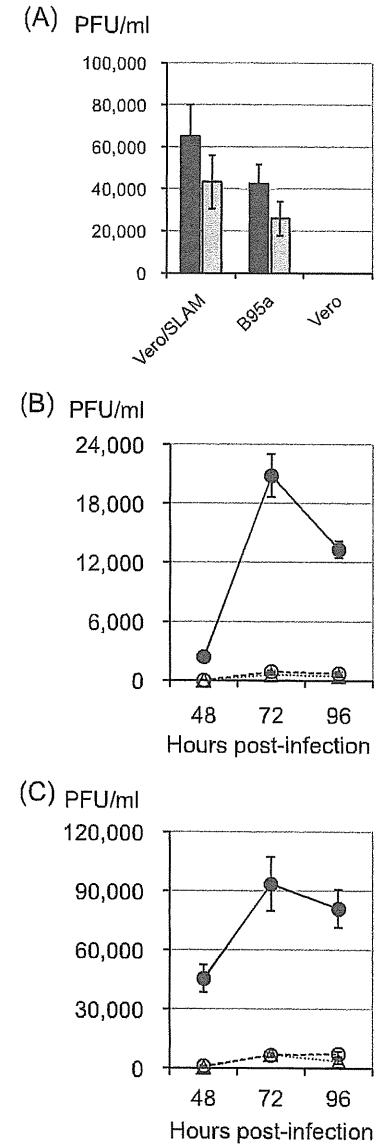

FIG. 2. (A) Plaque titration of the CD-VLP of recombinant MV containing the M gene of either OSA2FrV (IC/OSA2FrVM; black bars) or OSA2FrB (IC/OSA2FrBM; gray bars). Three different kinds of cell lines were used for the titration. The means ± standard deviations for triplicate samples are shown. (B and C) Growth kinetics of the recombinant MVs containing the M gene. B95a cells were infected with each recombinant MV at a multiplicity of infection of 0.01 PFU/cell. At indicated time points, culture fluids were collected, an equal volume of medium was added, and cells were frozen and thawed once, clarified by centrifugation, and then titrated. Filled circles, IC323; open triangles, IC/OSA2FrBM; open circles, IC/OSA2FrVM. Data shown are for infectious cell-free viruses released into the culture medium (B) and cell-associated viruses prepared by the freezing and thawing of infected cells (C).

TABLE 1. Inocula of recombinant viruses containing the M gene of the SSPE Osaka-2 strain and neurovirulence in hamsters

Virus	Expt no.	Titer (PFU) by cell type[a]		Incidence of disease[b]
		Vero	B95a	
IC323	1	<0.5	850	0/6
	2	<0.5	11,500	0/4
OSA2FrVM	1	<0.5	3,150	0/5
OSA2FrBM	1	<0.5	2,250	0/5

[a] Titer (PFU) of the inoculated virus (50 μl/brain) was determined either on Vero cells or on B95a cells.

[b] Number of diseased hamsters/number of inoculated hamsters. Hamsters showed no symptoms of disease onset after intracerebral inoculation until the time of death or sacrifice at the terminal stage, with one exception. Hamster 216 died 16 days after intracerebral inoculation without any neurological symptoms except for continuous weight loss, and the death was considered unrelated to the recombinant virus infection.

Recombinant MV containing the F or H gene of the SSPE Osaka-2 strain was defective in infectious cell-free virus production. Genes coding for the two envelope glycoproteins are also frequently mutated in most SSPE strains though the extent of the mutation occurring in the F and H genes is less significant than that occurring in the M gene. To ascertain the effects of the mutations developed in the F and H genes on the functions of their proteins, we prepared recombinant viruses containing either the F or H gene or both genes of the SSPE Osaka-2/FrV strain (Fig. 1). The recombinant viruses were prepared by a method similar to that described above for the viruses containing the M gene. B95a cells were infected with the CD-VLP stock, and the culture medium was harvested at 72 h p.i. and titrated to quantify infectious cell-free virus production (Fig. 3). The production level of virus carrying the F or H gene (IC/OSA2F and IC/OSA2H, respectively) was 8.3% ± 2.4% or 14.7% ± 4.6%, respectively, of that of the parental IC323 virus. Cell-free virus production by the IC/OSA2FH virus, the F and H double mutant, was further restricted and decreased to 3.3% ± 20.6% of that produced by the IC323 virus. The yield of intracellular viruses prepared by freezing and thawing of infected cells was also low (Fig. 3). The results indicated that the amino acid substitutions developed in the Osaka-2 F and H proteins affected virus particle production.

Recombinant MV containing the F gene of the SSPE Osaka-2 strain infects cell lines of neural origin. To determine whether the recombinant viruses containing the F or H gene of the Osaka-2 strain have different cell tropisms, a series of cell lines of different origins were used, including cell lines of neural origin, IMR-32 and SK-N-SH from human neuroblastoma, A172 from human oligodendroglioma, and U-251 from human astrocytoma (Table 2). As expected, all the viruses infected SLAM-positive cell lines such as B95a and CHO/SLAM cells and induced syncytia, whereas no virus infected CD46-positive CHO/CD46 cells. Recombinant viruses containing the F gene of the Osaka-2 strain (IC/OSA2FH and IC/OSA2F) infected Vero, IMR-32, and SK-N-SH cell lines and induced syncytia. A172 cells were also positive, but U-251 cells were negative by the immunofluorescence test. In contrast, recombinant viruses containing the H gene of the Osaka-2 strain (IC/OSA2H) had a similar cell tropism to the wild-type IC323 virus. These results suggest that the F protein of the Osaka-2 strain played a key role in the tropism and syncytium formation of some types of cells of neural origin.

The F and H genes of the SSPE Osaka-2 strain are determinants of neurovirulence. To test the neurovirulence of the recombinant viruses, IC323-based viruses containing either the F or H gene or both genes of the SSPE Osaka-2 strain (IC/OSA2F, IC/OSA2H, or IC/OSA2FH, respectively) were inoculated into hamster brains (Table 3). All the hamsters inoculated with the IC/OSA2FH virus (4,250 PFU/brain as assayed by B95a cells) developed neurological signs such as hyperactivity and seizures 3 or 4 days postinfection (p.i.). The symptoms observed in the hamsters were similar to those of animals inoculated with the parental Osaka-2 strain. All of these hamsters died or became moribund within 2 days after the onset of symptoms. The hamsters inoculated with the IC/OSA2F virus (2,450 PFU/brain as assayed by B95a cells) also showed neurological signs within 4 days p.i. and died or became moribund within 3 days after the onset. Smaller amounts of the IC/OSA2F virus (245 or 25 PFU/brain as assayed by B95a cells) induced the disease in three out of four hamsters, but one or two of the hamsters recovered.

The hamsters inoculated with the IC/OSA2H virus (2,900 PFU/brain as assayed by B95a cells) also showed neurological signs, and two of the four hamsters died; the minimum amount of the IC/OSA2H virus that could kill a hamster was 29 PFU/brain. However, the incidence of neurovirulence was much lower than that of the hamsters inoculated with the IC/OSA2F virus, and the incubation period was longer and varied.

Recombinant MVs containing the envelope genes of the SSPE Osaka-2 strain affected pyramidal cells in fields CA1 through CA3 of the hippocampus. Some of the hamsters inoculated with the recombinant MVs were sacrificed on the verge of death or at the endpoint of the observation, and hematoxylin and eosin-stained sections of the brains were prepared (Fig. 4). Hamsters inoculated with the IC323 virus

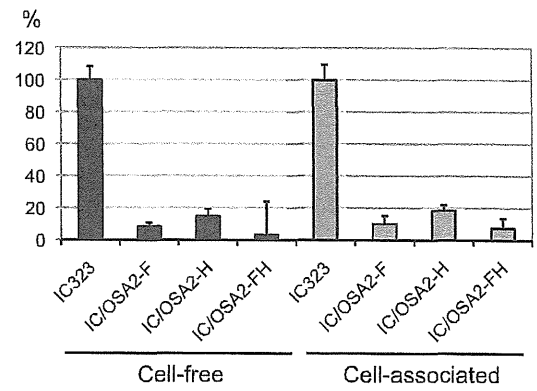

FIG. 3. Infectious cell-free virus production by the recombinant MVs. B95a cells were infected with each recombinant MV at a multiplicity of infection of 0.01 PFU/cell. At 72 h p.i., the virus released into the culture fluid (cell-free) or the cell-associated virus prepared by the freezing and thawing of infected cells (cell-associated) was titrated on B95a cells. The virus titer in cells infected with the IC323 strain was set to 100%. Bars indicate the means with standard deviations for triplicate samples.

TABLE 2. Susceptibility of various cell lines to recombinant MV

Cell line	Detection of virus[a]							
	IC323		IC/OSA2FH		IC/OSA2F		IC/OSA2H	
	Syncytia	IFA	Syncytia	IFA	Syncytia	IFA	Syncytia	IFA
B95a	+	+	+	+	+	+	+	+
Vero	−	+	+	+	+	+	−	−
IMR-32	−	−	+	+	+	+	−	−
SK-N-SH	−	+	+	+	+	+	−	−
A172	−	−	−	+	−	+	−	−
U-251	−	−	−	−	−	−	−	−
CHO/CD46	−	−	−	−	−	−	−	−
CHO/SLAM	+	+	+	+	+	+	+	+

[a] Determined by the presence (+) or absence (−) of syncytium formation and of immunofluorescent staining. IFA, immunofluorescence assay.

had no lesions throughout the brain (Fig. 4A), whereas severe lesions were found in fields CA1 through CA3 of the hippocampi of hamsters inoculated with the IC/OSA2FH (Fig. 4B) or IC/OSA2F (Fig. 4C) virus. The regions were equally affected in both hemispheres, and the pyramidal cells showed necrosis. The hamsters inoculated with IC/OSA2H (Fig. 4D) that developed neurological signs and were sacrificed showed minimal lesions with necrotic neurons in the CA1 field of the hippocampus. These histopathological observations and the incidence of neurovirulence indicate the relative importance of the F gene for the effective spread in the brain.

The extracellular domain of the F protein is responsible for neurovirulence in hamsters. We previously demonstrated syncytium formation in Vero cells when the F protein from the SSPE strain was coexpressed with the H protein from any MV strain (6). The region of the F protein responsible for syncytium formation was assigned principally to the extracellular domain though the cytoplasmic domain also played a role to some extent in the enhanced fusogenic activity. To investigate the differential effects of the amino acid substitutions in each domain in the infected cells, additional recombinant viruses were prepared. Recombinant viruses (IC/F:OSA2-ext and IC/F:OSA2-cyt) were recovered (Fig. 5) from full-length plasmids containing a chimeric F gene either of the extracellular or cytoplasmic domain, respectively, of the Osaka-2 strain. The IC/F:OSA2-ext virus infected and induced syncytia in Vero cells at a rate similar to that of the IC/OSA2F virus, whereas the IC/F:OSA2-cyt virus did not infect Vero cells (data not shown). Both the IC/F:OSA2-ext and IC/F:OSA2-cyt viruses

TABLE 3. Inocula of recombinant viruses containing the F or H gene of the SSPE Osaka-2 strain and neurovirulence in hamsters

Virus	Expt no.	Titer (PFU) by cell type[a]		No. of days to onset of disease (survival time [days])[b]	Incidence of disease[c]
		Vero	B95a		
IC/OSA2FH	1	25	4,250	3 (2), 3 (2), 3 (2*), 4 (1*), 4 (2*), 4 (2*)	6/6
IC/OSA2F	1	150	2,450	3 (2*), 3 (2*), 3 (3), 3 (3*), 3 (3*), 4 (2)	6/6
	2	150	2,450	3 (3), 3 (3*)	2/2
		15	245	5 (2), 5 (2*), 20 (−), − (−)	3/4
		1.5	25	5 (121), 6 (−), 7 (3), − (−)	3/4
IC/OSA2H	1	<0.5	750	9 (8*), 26 (1*), − (−), − (−), − (−),− (−)	2/6
	2	<0.5	2,900	7 (4*), 11 (3*), − (−), − (−)	2/4
		<0.05	290	15 (3), − (−), − (−), − (−)	1/4
		<0.005	29	23 (3), − (−), − (−), − (−)	1/4
IC323	1		2,000	− (−), − (−), − (−), − (−), − (−), − (−)	0/6
IC/F:OSA2F	1	122	2,000	3 (3*), 3 (3*)	2/2
IC/F:OSA2ext	1	12	2,000	3 (1), 3 (2), 3 (2), 4 (2)	4/4
IC/F:OSA2cyt	1	0.16	2,000	− (−), − (−), − (−), − (−)	0/4
	2	2.0	25,000	− (−), − (−), − (−), − (−)[d]	0/4
IC/F:L197I	1	0.1	2,000	− (−), − (−), − (−), − (−)	0/4
IC/F:Y442D	1	5	2,000	4 (−), 4 (−), 4 (−), 5 (41), 5 (−),− (−)	5/6
IC/F:T461I	1	110	2,000	4 (2*), 4 (4), 4 (5), 4 (−), 5 (1*), 5 (4)	6/6
IC/F:E478G	1	<0.01	2,000	− (−), − (−), − (−), − (−)	0/4

[a] The titer of the inoculated virus (50 μl/brain) was determined in either Vero cells or B95a cells.

[b] Number of days from intracerebral inoculation to the onset of the disease is shown (−, no symptoms). In parentheses, the number of days from onset of disease to death or sacrifice at the terminal stage, indicated by an asterisk, is shown (−, animal did not die).

[c] Number of diseased hamsters/number of inoculated hamsters.

[d] Hamster 248 died 21 days after intracerebral inoculation without any neurological symptoms, and the virus was not recovered; the death was considered unrelated to the recombinant virus infection.

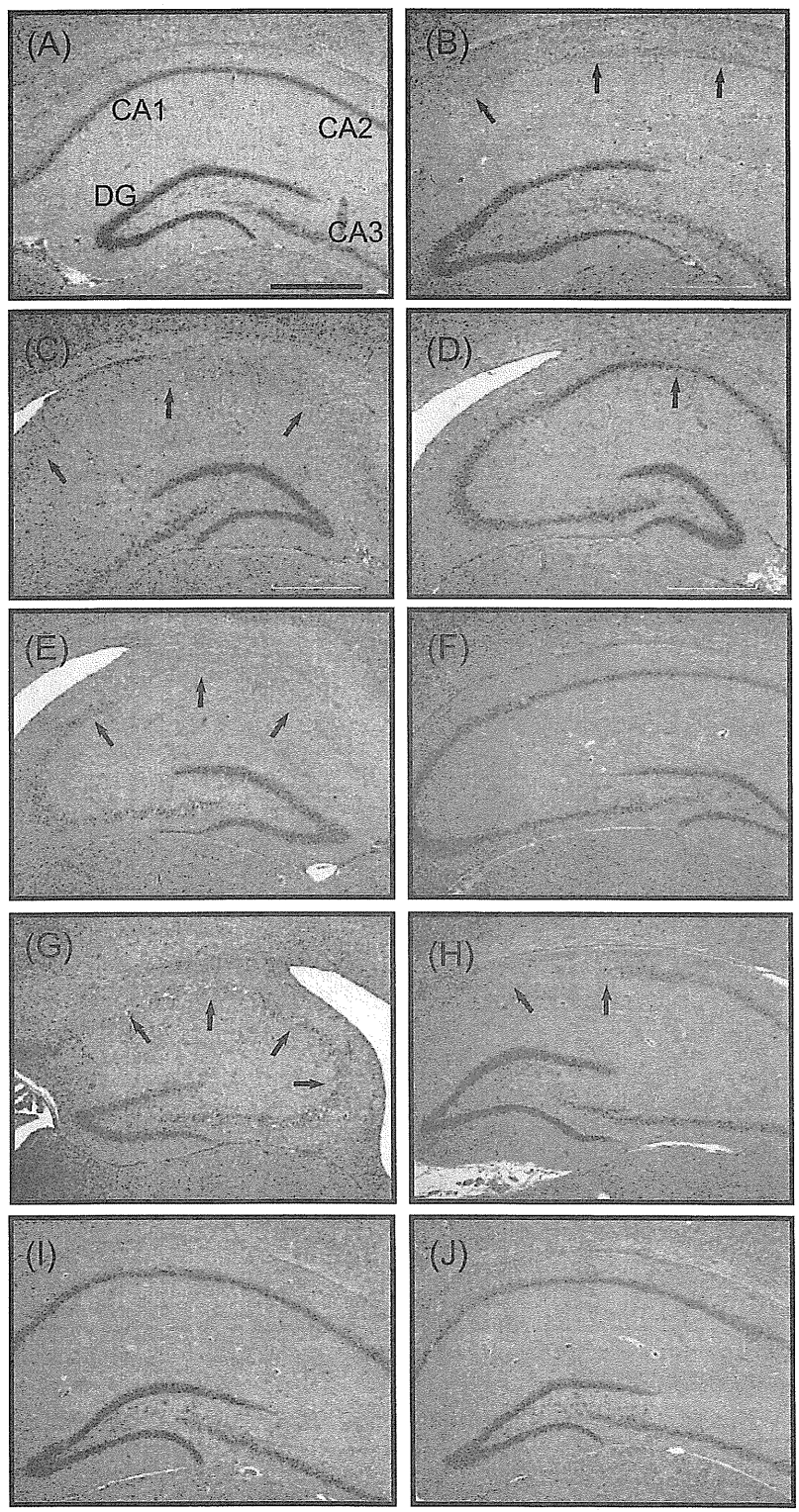

FIG. 4. Histopathological findings of the hippocampus. Neuronal loss and degenerated neurons were observed with different extents of severity in fields CA1 through CA3 of hamsters inoculated with the IC/OSA2FH, IC/OSA2F, IC/OSA2H, IC/F:OSA2F-ext, IC/F:T461I, and IC/F:Y442D (B to E, G, and H), whereas no lesion was detected in the brain of the hamsters inoculated with the wild-type IC323, IC/F:OSA2-cyt, IC/F:L197I, or IC/F:E478G virus (A, F, I, and J). In hamsters inoculated with the IC/OSA2H virus (D), neuronal damage was restricted to the CA1 field of the hippocampus. Proliferation and activation of astroglia and microglia were also noted in the affected areas. Inoculated viruses were the following: IC323 (hamster 262; showed no symptoms and was sacrificed at 70 days p.i.) (A); IC/OSA2FH (hamster 290; showed symptoms at 4 days

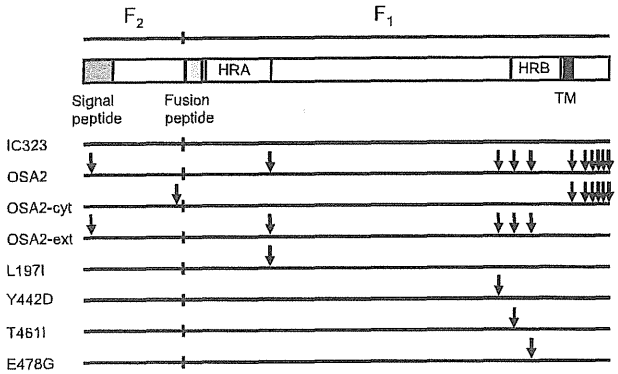

FIG. 5. Schematic diagram of the MV F protein and constructs. HRA and HRB, two highly conserved heptad repeat domains, are shown; regions of signal peptide and fusion peptide are indicated as shaded boxes. TM, transmembrane domain (black box). Arrows indicate amino acids different from the those of the IC323 strain. For the F and H coexpression experiments by transfection, the fragments were inserted into a eukaryotic expression vector, pME18S. For the recombinant MV constructions, plasmids were prepared by replacing the whole F gene fragment from the basic plasmid containing the IC323 viral genome.

produced infectious cell-free virus at approximately 5% of the IC323 virus level (data not shown).

The IC/F:OSA2-ext and IC/F:OSA2-cyt viruses were inoculated into hamster brains at a titer of 2,000 PFU per brain (Table 3). Hamsters inoculated with the IC/F:OSA2-ext virus developed neurological signs such as general seizures 3 or 4 days p.i. and died 1 or 2 days after the onset of seizures, whereas hamsters inoculated with the IC/F:OSA2-cyt virus showed no symptoms. In a further study, four hamsters that were inoculated with the larger amount of the IC/F:OSA2-cyt virus (25,000 PFU per brain) did not develop the disease. Therefore, the extracellular domain of the F protein of the Osaka-2 strain is responsible for neurovirulence in hamsters.

A single amino acid substitution in the extracellular domain of the F protein is responsible for enhanced fusogenicity in Vero cells and neurovirulence in hamsters. Because I10V, an isoleucine-to-valine substitution at amino acid 10 in the N-terminal region of the F protein, is included in the signal peptide that is deleted after synthesis, only four amino acids, L197I, Y442D, T461I, and E478G, are different between the IC323 and the Osaka-2 strains in the extracellular domain of the F protein. We then prepared four additional mutant plasmids that expressed the F protein with a single amino acid substitution. The resulting F plasmids were individually coexpressed with the IC323 H protein in B95a or Vero cells, and the ability to induce syncytium formation (Fig. 6) was examined. As expected, all four mutants induced syncytia in B95a cells within 24 h posttransfection, indicating that these F mutant proteins were functionally expressed on the cell surface (data not shown). On the other hand, only the T461I mutant efficiently induced syncytia in Vero cells at 24 h posttransfection (Fig. 6C). The Y442D mutant also induced syncytia, but it took 72 h or more to make small ones (data not shown).

Four recombinant viruses containing the F gene that expressed the F protein with a single amino acid substitution found in the extracellular domain of the Osaka-2 F protein were recovered (Fig. 5) and inoculated into hamster brain. Hamsters inoculated with the virus containing the T461I F protein mutation (IC/F:T461I) developed neurological signs 4 or 5 days p.i. and died 4 or 5 days after the onset of signs (Table 3). Hamsters inoculated with the IC/F:Y442D virus also developed neurological signs 4 or 5 days p.i. but recovered and survived for at least 24 weeks. Two other mutant viruses (IC/F:L197I and IC/F:E478G virus) did not produce any neurological signs.

Some of the dead or dying hamsters were subjected to histopathological examination (Fig. 4). As found in the brains of hamsters inoculated with the IC/OSA2FH or IC/OSA2F virus, severe lesions were found around the CA1 field of the hippocampus of the brains from the hamsters inoculated with the IC/F:OSA2-ext or IC/F:T461I virus (Fig. 4E and G). Old lesions with neuronal loss and astrogliosis were documented in the CA1 field of the hippocampus of the brain from hamsters inoculated with the IC/F:Y442D virus (Fig. 4H). In contrast, no lesion was found in the brains of hamsters inoculated with the IC/F:OSA2-cyt, IC/F:L197I, or IC/F:E478G virus (Fig. 4F, I, and J). Therefore, the severity of the lesions correlated with neurovirulence.

DISCUSSION

SSPE strains of MV contain numerous mutations, especially in the M, F, and H genes, which result in structural alterations of the proteins encoded by these genes. It is important to ascertain whether these changes are simple accumulations during long-term persistence of the virus or changes necessary for effective virus spread in the brain. Because SLAM, the primary entry receptor for wild-type MV, is not expressed on neural cells and because basically SSPE strains do not use CD46 as an alternative receptor (28, 63), it is reasonable to speculate that changes or adaptations that use an unidentified receptor are introduced in the envelope proteins. The recent development of MV rescue system technology allowed us to identify the molecular determinant(s) of MV responsible for the phenotypic change *in vitro* and for neurovirulence. Cathomen et al. first described the role of mutations found in SSPE strains by

p.i. and was sacrificed at 6 days p.i.) (B); IC/OSA2F (hamster 176; showed symptoms at 3 days p.i. and was sacrificed at 6 days p.i.) (C); IC/OSA2H (hamster 187; showed symptoms at 7 days p.i. and was sacrificed at 12 days p.i.) (D); IC/F:OSA2-ext (hamster 237; showed symptoms at 3 days p.i. and died at 5 days p.i.) (E); IC/F:OSA2-cyt (hamster 245; showed no symptoms and was sacrificed at 280 days p.i.) (F); IC/F:T461I (hamster 275; showed symptoms at 5 days p.i. and was sacrificed at 6 days p.i.) (G); IC/F:Y442D (hamster 268; showed symptoms at 4 days p.i. and was sacrificed at 168 days p.i.) (H); IC/F:L197I (hamster 258; showed no symptoms and was sacrificed at 70 days p.i.) (I); IC/F:E478G (hamster 278; showed no symptoms and was sacrificed at 70 days p.i.) (J). CA1, CA2, CA3, and DG (dentate gyrus) fields are indicated in panel A. Scale bar, 500 μm. Panels A, B, and G to J show the hippocampus area of the left hemisphere, and panels C to F show the hippocampus area of the right hemisphere of the brain. The arrows indicate the abnormal appearance of fields CA1 through CA3 due to the necrosis of pyramidal cells.

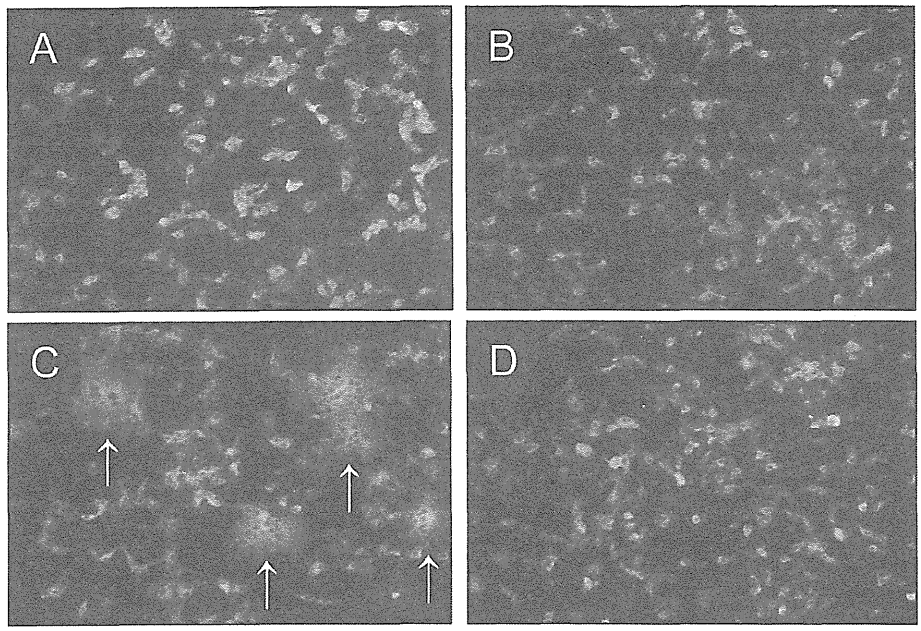

FIG. 6. Syncytium formation induced by a different kind of mutant F protein. Vero cells were cotransfected with plasmid DNA encoding the H and F proteins of MV. The H gene was derived from the IC323 strain while the F gene was from one of the mutant F genes. At 24 h p.i., cells were fixed and stained with a monoclonal antibody to the H protein and fluorescein isothiocyanate-conjugated anti-mouse antibody. (A) IC/F:L197I. (B) IC/F:Y442D. (C) IC/F:T461I. (D) IC/F:E478G. Arrows in panel C indicate syncytia formed in cells cotransfected with the F gene containing the T461I substitution. No syncytia were found in cells cotransfected with other F genes.

adapting the recombinant MV system (10, 11). In a similar system, Patterson et al. also described the role of the mutation in the M gene (52). However, these experiments used a recombinant MV system based on the Edmonston strain (10, 11, 52) and CD46 transgenic mice (10, 52), and hence CD46 would be used as the receptor for the infection. Therefore, we generated recombinant viruses containing SSPE genes from a vector plasmid based on the wild-type MV IC323 strain (65). In this study, we analyzed the functional alterations of the envelope-associated proteins both *in vitro* and *in vivo*.

As previously reported (10, 52), recombinant MVs in which the M gene was deleted or replaced by the hypermutated M gene from SSPE strains were infectious but showed reduced productivity of the extracellular cell-free virion. We also generated infectious recombinant viruses containing the M gene of the Osaka-2 strain, and the virus-infected cells showed a nonproductive nature. Although the hypermutation of the M gene resulting in the defective expression of the M protein is the most characteristic feature in the genome of many SSPE strains, including the Osaka-2 strain, replacement of the M gene alone did not confer a neurovirulent phenotype in hamsters. Rather, it is possible to consider the M gene mutation as a contributing factor to attenuation. It should be noted that a matrix-less MV lost acute pathogenicity but penetrated more deeply into the brain parenchyma than the Edmonston MV in mice expressing the human receptor CD46 and defective for the interferon type I system (10); and the recombinant MV containing the biased hypermutated M gene of the Biken strain, from which the defective M protein was produced, induced prolonged infection occurring as long as 30 to 50 days after that caused by MV (52). We do not exclude the possibility that the defect of the M protein in the Osaka-2 strain makes some contribution to its persistence in the brain.

Experiments using the transient coexpression of the F and H proteins demonstrated that the extracellular domain of the F protein was responsible for efficient syncytium formation in SLAM-negative Vero cells as well as in cell lines expressing SLAM or CD46 (6). The region responsible for the enhanced fusogenicity was further narrowed to the level of a single amino acid in the current study. Substitution of a single amino acid (T461I) was sufficient for enhancement of fusion activity. This residue is located in the heptad repeat B (HRB) domain, which is adjacent to the transmembrane domain (20, 35). The HRB domain is thought to be involved in the conformational change during the fusion process to make a six-helix bundle structure with the heptad repeat A (HRA) domain, which is adjacent to the fusion peptide (reviewed in reference 36). Although fusogenic activity was lower than that caused by the T461I substitution, another amino acid change, Y442D, also induced syncytia in Vero cells. Doyle et al. (17) reported the alteration of fusogenic activity of mutant F proteins with amino acid substitutions at positions 94, 367, and 462. Okada et al. (49) also described the enhanced fusogenicity resulting from a single G464W substitution in the F protein, which was developed in a Vero cell-adapted wild-type T11 strain. These results suggested that the conformational change of the F protein due to an amino acid substitution at a different site could result in a similar enhancement of fusion activity. We previously described the effects of amino acid substitutions in the F protein from three SSPE strains (Osaka-1, Osaka-2, and Osaka-3) on syncytium formation in Vero cells. These three SSPE strains replicate and induce syncytia in Vero cells, and the SSPE F

protein was responsible for syncytium formation. The T461I substitution was found in the F protein of the Osaka-3 strain as well as in the Osaka-2 strain. However, substitutions found in the F protein of the Osaka-1 strain do not overlap with those in the Osaka-2 strain. It is possible that other substitution(s) or combinations could induce similar conformational changes in the protein and could result in the same phenotype, i.e., enhanced fusion. We are currently preparing recombinant viruses containing the F and H genes from the Osaka-1 strain to verify the idea suggested by the results obtained from the analysis of the Osaka-2 strain.

A series of recombinant viruses containing mutations in the F gene were generated on the IC323 wild-type strain background. Expression of the F gene with a single T461I substitution in the F protein (IC/F:T461I virus) was sufficient to induce lethal encephalopathy in hamsters. Expression of the F gene with a Y442D substitution in the F protein (IC/F:Y442D virus) also induced severe neurological symptoms though these hamsters recovered quickly from the disease. Considering that the Y442D substitution induced syncytium formation less efficiently than the T461I substitution in the F and H cotransfection experiments, there is a good correlation between the extent of the fusion activity *in vitro* and the severity of neurovirulence in hamsters. As previously described (10, 11), MV bearing an F protein with a shortened cytoplasmic tail induced enhanced cell fusion. The virus lost acute pathogenicity but penetrated more deeply into the brain parenchyma than the Edmonston MV in the CD46-transgenic, interferon type I-deficient mice. The result indicated that defects in the cytoplasmic tail of the F protein resulted in attenuation of MV neurovirulence in mice. The role of the F gene in neurovirulence of other viruses has been reported. The F gene of rodent brain-adapted mumps virus was a major determinant of neurovirulence in neonatal Lewis rats (40). Lemon et al. showed that expression of the F gene alone of the neurovirulent strain was sufficient to induce significant levels of hydrocephalus in the animals. However, there was no correlation between fusogenicity and neurovirulence, and the mechanism whereby the mumps virus F protein modulates neurovirulence remains unknown. The direct correlation of enhanced fusogenicity and neurovirulence of the Osaka-2 strain will be evaluated by similar experiments with the Osaka-1 strain, the F protein of which has different substitutions, as discussed above.

In addition to the F protein, the H protein contributed to neurovirulence to some extent. Some (30 to 50%) of the hamsters inoculated with the recombinant virus expressing the H protein of the Osaka-2 strain (IC/OSA2H virus) developed the same neurological symptoms as those inoculated with the virus containing the Osaka-2 F gene (IC/OSA2F virus). The incidence was much lower in hamsters inoculated with the IC/OSA2H virus than in those inoculated with the IC/OSA2F virus, and the onset was delayed. This minor but definite contribution of the H gene to neurovirulence was masked by the major contribution of the F gene in the hamsters inoculated with the IC/OSA2FH virus. Further study will be needed in order to differentiate the role of the H protein in neurovirulence. Duprex et al. described the role of the H gene of the CAM/RB strain, a rodent brain-adapted MV, in neurovirulence in newborn mice (18). Further study revealed that the combination of two amino acid substitutions (R195G and N200S) in the stem 2 region of MV H protein determined neurovirulence (44). However, these two amino acid substitutions are unique to the CAM/RB strain and are not found in SSPE strains. Therefore, the role and mechanism of the Osaka-2 H protein in neurovirulence could be different. It should be noted that the recombinant virus containing the CAM/RB-H gene replicated in the brains of mice to a lesser extent than the parental CAM/RB virus, indicating the requirement of other genes for full neurovirulence. This is consistent with our result of minimum neurovirulence in the recombinant virus expressing the Osaka-2 H protein in hamsters. Further investigation is required to address the question of which amino acid substitution(s) is responsible for neurovirulence.

The mechanism of the restricted production of infectious cell-free virus by the SSPE F- and H-containing virus is largely unknown. It is possible that the interaction between the F and H proteins with the M protein is restricted because of the alteration of the cytoplasmic domain of the envelope glycoproteins. Cathomen et al. suggested the association of M with the cytoplasmic tails of the glycoproteins might negatively influence their fusion efficiency (11). However, the restricted production of infectious cell-free virus by the mutant F protein that contained only the extracellular domain of the Osaka-2 strain cannot be explained by this mechanism. Our preliminary data indicated that even a single substitution in the extracellular domain could greatly alter cell-free virus production (unpublished observations). The F protein is highly conserved, and only one or two amino acid differences are found among wild-type MV strains. This implies the elimination of viruses containing a mutant F protein that affects the production of infectious virions. It is possible that such mutations found in SSPE strains are allowed or selected in a specific environment such as the brain.

The mechanism of the spread of MV in the brain is poorly understood. A hypothesis of transsynaptic spread of MV in neurons without interaction between the H protein and the host cellular receptor was proposed (38). Further investigation suggested that neurokinin-1 (NK-1), a member of the neurotachykinin family of G protein-coupled neurotransmitter receptors, served as a receptor for the MV F protein (43). Because the fusion-inhibitory peptide (FIP; Z-D-Phe-L-Phe-Gly) is known to inhibit fusion by paramyxovirus (54, 55) and because the tripeptide sequence is identical to the active site of substance P, a ligand for NK-1, it is possible that the SSPE F protein is more effective for microfusion at the synaptic cleft. However, it is equally possible that the virus spreads by microfusion via a specific interaction between the H protein and an unidentified host cellular receptor at the synapse. It should be noted that syncytium formation was observed in the CA1 field of one hamster brain that was inoculated with the Osaka-2 strain (29). In a study of MV spread in neurons using rat hippocampal slice culture (21), MV showed a retrograde spread from CA1 to CA3 pyramidal cells. This observation is consistent with the result we observed in the hippocampal region, which showed that the CA1 field was the most affected and that the CA2 and CA3 fields were also affected in severe cases. The apparent target region of the recombinant virus containing the SSPE H gene was also the CA1. Because binding of the H protein with the host cellular receptor is usually

required for the induction of a conformational change in the F protein, the differential role of the H protein in virus spread in the brain should be clarified. To understand this, substitutions appearing in the SSPE H protein should be evaluated individually in relation to the interaction with the yet unidentified receptor(s) on Vero cells (5), epithelial cells (41, 67, 68), and neural cells, as well as the known receptors SLAM and CD46.

In conclusion, our findings indicate that the F gene of the Osaka-2 strain of MV is a major determinant of neurovirulence, regardless of whether a specific interaction between the H protein and the host cellular receptor is involved. A single amino acid substitution in the F protein is sufficient for neurovirulence. Studies of recombinant viruses containing the F gene with mutations found in different SSPE strains are necessary to understand the relationship between the increased fusogenicity and neurovirulence. In addition, identification of an unidentified alternative receptor in Vero and neural cells will provide new insights into the mechanism of MV spread in the brain and the pathogenesis of SSPE and open a way to develop a novel therapy.

ACKNOWLEDGMENTS

We thank Y. Murakami and Y. Yanagi for providing cell lines and B. Moss for vaccinia virus vTF7-3. We also thank E. Nishiguchi and R. Tanaka for technical assistance and the staff of the Central Laboratory of Osaka City University Medical School for technical support.

This work was supported by a Grant-in-Aid for Scientific Research (number 19591216) from the Ministry of Education, Science, Sports, and Culture of Japan.

REFERENCES

1. **Albrecht, P., and H. P. Schumacher.** 1971. Neurotropic properties of measles virus in hamsters and mice. J. Infect. Dis. **124**:86–93.
2. **Albrecht, P., T. Burnstein, M. J. Klutch, H. T. Hicks, and F. A. Ennis.** 1977. Subacute sclerosing panencephalitis: experimental infection in primates. Science **195**:64–66.
3. **Ayata, M., A. Hirano, and T. C. Wong.** 1989. Structural defect linked to nonrandom mutations in the matrix gene of Biken strain subacute sclerosing panencephalitis virus defined by cDNA cloning and expression of chimeric genes. J. Virol. **63**:1162–1173.
4. **Ayata, M., K. Hayashi, T. Seto, R. Murata, and H. Ogura.** 1998. The matrix gene expression of subacute sclerosing panencephalitis (SSPE) virus (Osaka-1 strain): a comparison of two sibling viruses isolated from different lobes of an SSPE brain. Microbiol. Immunol. **42**:773–780.
5. **Ayata, M., K. Komase, M. Shingai, I. Matsunaga, Y. Katayama, and T. C. Wong.** 2002. Mutations affecting transcriptional termination in the P gene end of subacute sclerosing panencephalitis viruses. J. Virol. **76**:13062–13068.
6. **Ayata, M., M. Shingai, X. Ning, M. Matsumoto, T. Seya, S. Otani, T. Seto, S. Ohgimoto, and H. Ogura.** 2007. Effect of the alterations in the fusion protein of measles virus isolated from brains of patients with subacute sclerosing panencephalitis on syncytium formation. Virus Res. **130**:260–268.
7. **Baringer, J. R., and J. F. Griffith.** 1970. Experimental measles virus encephalitis. A light, phase, fluorescence, and electron microscopic study. Lab. Invest. **23**:335–346.
8. **Billeter, M. A., R. Cattaneo, P. Spielhofer, K. Kaelin, M. Huber, A. Schmid, K. Baczko, and V. ter Meulen.** 1994. Generation and properties of measles virus mutations typically associated with subacute sclerosing panencephalitis. Ann. N. Y. Acad. Sci. **724**:367–377.
9. **Byington, D. P., and K. P. Johnson.** 1972. Experimental subacute sclerosing panencephalitis in the hamster: correlation of age with chronic inclusion-cell encephalitis. J. Infect. Dis. **126**:18–26.
10. **Cathomen, T., B. Mrkic, D. Spehner, R. Drillien, R. Naef, J. Pavlovic, A. Aguzzi, M. A. Billeter, and R. Cattaneo.** 1998. A matrix-less measles virus is infectious and elicits extensive cell fusion: consequences for propagation in the brain. EMBO J. **17**:3899–3908.
11. **Cathomen, T., H. Y. Naim, and R. Cattaneo.** 1998. Measles viruses with altered envelope protein cytoplasmic tails gain cell fusion competence. J. Virol. **72**:1224–1234.
12. **Cattaneo, R., A. Schmid, G. Rebmann, K. Baczko, V. ter Meulen, W. J. Bellini, S. Rozenblatt, and M. A. Billeter.** 1986. Accumulated measles virus mutations in a case of subacute sclerosing panencephalitis: interrupted matrix protein reading frame and transcription alteration. Virology **154**:97–107.
13. **Cattaneo, R., G. Rebmann, A. Schmid, K. Baczko, V. ter Meulen, and M. A. Billeter.** 1987. Altered transcription of a defective measles virus genome derived from a diseased human brain. EMBO J. **6**:681–688.
14. **Cattaneo, R., A. Schmid, M. A. Billeter, R. D. Sheppard, and S. A. Udem.** 1988. Multiple viral mutations rather than host factors cause defective measles virus gene expression in a subacute sclerosing panencephalitis cell line. J. Virol. **62**:1388–1397.
15. **Cattaneo, R., A. Schmid, D. Eschle, K. Baczko, V. ter Meulen, and M. A. Billeter.** 1988. Biased hypermutation and other genetic changes in defective measles viruses in human brain infections. Cell **55**:255–265.
16. **Cattaneo, R., A. Schmid, P. Spielhofer, K. Kaelin, K. Baczko, V. ter Meulen, J. Pardowitz, S. Flanagan, B. K. Rima, S. A. Udem, and M. A. Billeter.** 1989. Mutated and hypermutated genes of persistent measles viruses which caused lethal human brain diseases. Virology **173**:415–425.
17. **Doyle, J., A. Prussia, L. K. White, A. Sun, D. C. Liotta, J. P. Snyder, R. W. Compans, and R. K. Plemper.** 2006. Two domains that control prefusion stability and transport competence of the measles virus fusion protein. J. Virol. **80**:1524–1536.
18. **Duprex, W. P., I. Duffy, S. McQuaid, L. Hamill, S. L. Cosby, M. A. Billeter, J. Schneider-Schaulies, V. ter Meulen, and B. K. Rima.** 1999. The H gene of rodent brain-adapted measles virus confers neurovirulence to the Edmonston vaccine strain. J. Virol. **73**:6916–6922.
19. **Duprex, W. P., S. McQuaid, B. Roscic-Mrkic, R. Cattaneo, C. McCallister, and B. K. Rima.** 2000. In vitro and in vivo infection of neural cells by a recombinant measles virus expressing enhanced green fluorescent protein. J. Virol. **74**:7972–7979.
20. **Eckert, D. M., and P. S. Kim.** 2001. Mechanisms of viral membrane fusion and its inhibition. Annu. Rev. Biochem. **70**:777–810.
21. **Ehrengruber, M. U., E. Ehler, M. A. Billeter, and H. Y. Naim.** 2002. Measles virus spreads in rat hippocampal neurons by cell-to-cell contact and in a polarized fashion. J. Virol. **76**:5720–5728.
22. **Erlenhoefer, C., W. J. Wurzer, S. Löffler, S. Schneider-Schaulies, V. ter Meulen, and J. Schneider-Schaulies.** 2001. CD150 (SLAM) is a receptor for measles virus but is not involved in viral contact-mediated proliferation inhibition. J. Virol. **75**:4499–4505.
23. **Furukawa, K., M. Ayata, M. Kimura, T. Seto, I. Matsunaga, R. Murata, T. Yamano, and H. Ogura.** 2001. Hemadsorption expressed by cloned H genes from subacute sclerosing panencephalitis (SSPE) viruses and their possible progenitor measles viruses isolated in Osaka, Japan. Microbiol. Immunol. **45**:59–68.
24. **Griffin, D. E., J. Mullinix, O. Narayan, and R. Johnson.** 1974. Age dependence of viral expression: comparative pathogenesis of two rodent-adapted strains of measles virus in mice. Infect. Immun. **126**:690–695.
25. **Griffin, D. E.** 2007. Measles virus, p. 1551–1585. *In* D. M. Knipe, P. M. Howley, D. E. Griffin, R. A. Lamb, M. A. Martin, B. Roizman, and S. E. Straus (ed.), Fields Virology, 5th ed. Lippincott Williams & Wilkins, Philadelphia, PA.
26. **Hsu, E. C., F. Sarangi, C. Iorio, M. S. Sidhu, S. A. Udem, D. L. Dillehay, W. Xu, P. A. Rota, W. J. Bellini, and C. D. Richardson.** 1998. A single amino acid change in the hemagglutinin protein of measles virus determines its ability to bind CD46 and reveals another receptor on marmoset B cells. J. Virol. **72**:2905–2916.
27. **Hsu, E. C., C. Iorio, F. Sarangi, A. A. Khine, and C. D. Richardson.** 2001. CDw150(SLAM) is a receptor for a lymphotropic strain of measles virus and may account for the immunosuppressive properties of this virus. Virology **279**:9–21.
28. **Ishida, H., M. Ayata, M. Shingai, I. Matsunaga, Y. Seto, Y. Katayama, N. Iritani, T. Seya, Y. Yanagi, O. Matsuoka, T. Yamano, and H. Ogura.** 2004. Infection of different cell lines of neural origin with subacute sclerosing panencephalitis (SSPE) virus. Microbiol. Immunol. **48**:277–287.
29. **Ito, N., M. Ayata, M. Shingai, K. Furukawa, T. Seto, I. Matsunaga, M. Muraoka, and H. Ogura.** 2002. Comparison of the neuropathogenicity of two SSPE sibling viruses of the Osaka-2 strain isolated with Vero and B95a cells. J. Neurovirol. **8**:6–13.
30. **Iwata, K., T. Seya, H. Ariga, and S. Nagasawa.** 1994. Expression of a hybrid complement regulatory protein, membrane cofactor protein decay accelerating factor on Chinese hamster ovary: comparison of its regulatory effect with those of decay accelerating factor and membrane cofactor protein. J. Immunol. **152**:3436–3444.
31. **Johnson, K. P., and D. P. Byington.** 1971. Subacute sclerosing panencephalitis (SSPE) agent in hamsters. I. Acute giant cell encephalitis in newborn animals. Exp. Mol. Pathol. **15**:339–379.
32. **Johnson, K. P., and D. P. Byington.** 1977. Subacute sclerosing panencephalitis: animal models, p. 511–515. *In* D. Schlessinger (ed.), Microbiology. American Society for Microbiology, Washington DC.
33. **Katz, M., L. B. Rorke, W. S. Masland, G. B. Brodano, and H. Koprowski.** 1970. Subacute sclerosing panencephalitis: isolation of a virus encephalitogenic for ferrets. J. Infect. Dis. **121**:188–195.
34. **Kobune, F., H. Sakata, and A. Sugiura.** 1990. Marmoset lymphoblastoid cells as a sensitive host for isolation of measles virus. J. Virol. **64**:700–705.
35. **Lamb, R. A.** 1993. Paramyxovirus fusion: a hypothesis for changes. Virology **197**:1–11.

36. **Lamb, R. A., and T. S. Jardetzky.** 2007. Structural basis of viral invasion: lessons from paramyxovirus F. Curr. Opin. Struct. Biol. **17**:427–436.
37. **Lawrence, D. M., M. M. Vaughn, A. R. Belman, J. S. Cole, and G. F. Rall.** 1999. Immune response-mediated protection of adult but not neonatal mice from neuron-restricted measles virus infection and central nervous system disease. J. Virol. **73**:1795–1801.
38. **Lawrence, D. M., C. E. Patterson, T. L. Gales, J. L. D'Orazio, M. M. Vaughn, and G. F. Rall.** 2000. Measles virus spread between neurons requires cell contact but not CD46 expression, syncytium formation, or extracellular virus production. J. Virol. **74**:1908–1918.
39. **Lecouturier, V., J. Fayolle, M. Caballero, J. Carabana, M. L. Celma, R. Fernandez-Munoz, T. F. Wild, and R. Buckland.** 1996. Identification of two amino acids in the hemagglutinin glycoprotein of measles virus (MV) that govern hemadsorption, HeLa cell fusion, and CD46 downregulation: phenotypic markers that differentiate vaccine and wild-type MV strains. J. Virol. **70**:4200–4204.
40. **Lemon, K., B. K. Rima, S. McQuaid, I. V. Allen, and W. P. Duprex.** 2007. The F gene of rodent brain-adapted mumps virus is a major determinant of neurovirulence. J. Virol. **81**:8293–8302.
41. **Leonard, V. H. J., P. L. Sinn, G. Hodge, T. Miest, P. Devaux, N. Oezguen, W. Braun, P. B. McCray, Jr., M. B. McChesney, and R. Cattaneo.** 2008. Measles virus blind to its epithelial cell receptor remains virulent in rhesus monkeys but cannot cross the airway epithelium and is not shed. J. Clin. Invest. **118**:2448–2458.
42. **Li, L., and Y. Qi.** 2002. A novel amino acid position in hemagglutinin glycoprotein of measles virus is responsible for hemadsorption and CD46 binding. Arch. Virol. **147**:775–786.
43. **Makhortova, N., P. Askovich, C. E. Patterson, L. A. Gechman, N. P. Gerard, and G. F. Rall.** 2007. Neurokinin-1 enables measles virus trans-synaptic spread in neurons. Virology **362**:235–244.
44. **Moeller-Ehrlich, K., M. Ludlow, R. Beschorner, R. Meyermann, B. K. Rima, W. P. Duprex, S. Niewiesk, and J. Schneider-Schaulies.** 2007. Two functionally linked amino acids in the stem 2-region of measles virus haemagglutinin determine infectivity and virulence in the rodent central nervous system. J. Gen. Virol. **88**:3112–3120.
45. **Mrkic, B., J. Pavlovic, T. Rulicke, P. Volpe, C. J. Buchholz, D. Hourcade, J. P. Atkinson, A. Aguzzi, and R. Cattaneo.** 1998. Measles virus spread and pathogenesis in genetically modified mice. J. Virol. **72**:7420–7427.
46. **Nielsen, L., M. Blixenkrone-Moller, M. Thylstrup, N. J. V. Hansen, and G. Bolt.** 2001. Adaptation of wild-type measles virus to CD46 receptor usage. Arch. Virol. **146**:197–208.
47. **Ning, X., M. Ayata, M. Kimura, K. Komase, K. Furukawa, T. Seto, N. Ito, M. Shingai, I. Matusnaga, T. Yamano, and H. Ogura.** 2002. Alterations and diversity in the cytoplasmic tail of the fusion protein of subacute sclerosing panencephalitis virus strains isolated in Osaka, Japan. Virus Res. **86**:123–131.
48. **Ogura, H., M. Ayata, K. Hayashi, T. Seto, O. Matsuoka, H. Hattori, K. Tanaka, K. Tanaka, Y. Takano, and R. Murata.** 1997. Efficient isolation of subacute sclerosing panencephalitis virus from patient brains by reference to magnetic resonance and computed tomographic images. J. Neurovirol. **3**:304–309.
49. **Okada, H., M. Itoh, K. Nagata, and K. Takeuchi.** 2009. Previously unrecognized amino acid substitutions in the hemagglutinin and fusion proteins of measles virus modulate cell-cell fusion, hemadsorption, virus growth, and penetration rate. J. Virol. **83**:8713–8721.
50. **Oldstone, M. B., H. Lewicki, D. Thomas, A. Tishon, S. Dales, J. Patterson, M. Manchester, D. Homann, D. Naniche, and A. Holz.** 1999. Measles virus infection in a transgenic model: virus-induced immunosuppression and central nervous system disease. Cell **98**:629–640.
51. **Ono, N., H. Tatsuo, Y. Hidaka, T. Aoki, H. Minagawa, and Y. Yanagi.** 2001. Measles viruses on throat swabs from measles patients use signaling lymphocytic activation molecule (CDw150) but not CD46 as a cellular receptor. J. Virol. **75**:4399–4401.
52. **Patterson, J. B., T. I. Cornu, J. Redwine, S. Dales, H. Lewicki, A. Holz, D. Thomas, M. A. Billeter, and M. B. Oldstone.** 2001. Evidence that the hypermutated M protein of a subacute sclerosing panencephalitis measles virus actively contributes to the chronic progressive CNS disease. Virology **291**:215–225.
53. **Radecke, F., P. Spielhofer, H. Schneider, K. Kaelin, M. Huber, C. Dotsch, G. Christiansen, and M. A. Billeter.** 1995. Rescue of measles viruses from cloned DNA. EMBO J. **14**:5773–5784.
54. **Richardson, C. D., A. Scheid, and P. W. Choppin.** 1980. Specific inhibition of paramyxovirus and myxovirus replication by oligopeptides with amino acid sequences similar to those at the N-terminal of the F1 or HA2 viral polypeptides. Virology **105**:205–222.
55. **Richardson, C. D., and P. W. Choppin.** 1983. Oligopeptides that specifically inhibit membrane fusion by paramyxoviruses: studies on the site of action. Virology **131**:518–532.
56. **Rima, B. K., J. A. P. Earle, K. Baczko, V. ter Meulen, U. G. Liebert, C. Carstens, J. Carabana, M. Caballero, M. L. Celma, and R. Fernandez-Munoz.** 1997. Sequence divergence of measles virus haemagglutinin during natural evolution and adaptation to cell culture. J. Gen. Virol. **78**:97–106.
57. **Schmid, A., P. Spielhofer, R. Cattaneo, K. Baczko, V. ter Meulen, and M. A. Billeter.** 1992. Subacute sclerosing panencephalitis is typically characterized by alterations in the fusion protein cytoplasmic domain of the persisting measles virus. Virology **188**:910–915.
58. **Schneider, H., P. Spielhofer, K. Kaelin, C. Dötsch, F. Radecke, G. Sutter, and M. A. Billeter.** 1997. Rescue of measles virus using a replication-deficient vaccinia-T7 vector. J. Virol. Methods **64**:57–64.
59. **Schneider-Schaulies, J., V. ter Meulen, and S. Schneider-Schaulies.** 2003. Measles infection of the central nervous system. J. Neurovirol. **9**:247–252.
60. **Sellin, C. I., N. Davoust, V. Guillaume, D. Baas, M. F. Belin, R. Buckland, T. F. Wild, and B. Horvat.** 2006. High pathogenicity of wild-type measles virus infection in CD150 (SLAM) transgenic mice. J. Virol. **80**:6420–6429.
61. **Seto, T., M. Ayata, K. Hayashi, K. Furukawa, R. Murata, and H. Ogura.** 1999. Different transcriptional expression of the matrix gene of the two sibling viruses of the subacute sclerosing panencephalitis virus (Osaka-2 strain) isolated from a biopsy specimen of patient brain. J. Neurovirol. **5**:151–160.
62. **Shibahara, K., H. Hotta, Y. Katayama, and M. Homma.** 1994. Increased binding activity of measles virus to monkey red blood cells after long-term passage in Vero cell cultures. J. Gen. Virol. **75**:3511–3516.
63. **Shingai, M., M. Ayata, H. Ishida, I. Matsunaga, Y. Katayama, T. Seya, H. Tatsuo, Y. Yanagi, and H. Ogura.** 2003. Receptor use by vesicular stomatitis virus pseudotypes with glycoproteins of defective variants of measles virus isolated from brains of patients with subacute sclerosing panencephalitis. J. Gen. Virol. **84**:2133–2143.
64. **Sugita, T., K. Shiraki, S. Ueda, N. Iwa, H. Shoji, M. Ayata, and S. Kato.** 1984. Induction of acute myoclonic encephalopathy in hamsters by subacute sclerosing panencephalitis virus. J. Infect. Dis. **150**:340–347.
65. **Takeda, M., K. Takeuchi, N. Miyajima, F. Kobune, Y. Ami, N. Nagata, Y. Suzaki, Y. Nagai, and M. Tashiro.** 2000. Recovery of pathogenic measles virus from cloned cDNA. J. Virol. **74**:6643–6647.
66. **Takeda, M., S. Ohno, F. Seki, K. Hashimoto, N. Miyajima, K. Takeuchi, and Y. Yanagi.** 2005. Efficient rescue of measles virus from cloned cDNA using SLAM-expressing Chinese hamster ovary cells. Virus Res. **108**:161–165.
67. **Takeda, M., M. Tahara, T. Hashiguchi, T. A. Sato, F. Jinnouchi, S. Ueki, S. Ohno, and Y. Yanagi.** 2007. A human lung carcinoma cell line supports efficient measles virus growth and syncytium formation via a SLAM- and CD46-independent mechanism. J. Virol. **81**:12091–12096.
68. **Takeuchi, K., N. Miyajima, N. Nagata, M. Takeda, and M. Tashiro.** 2003. Wild-type measles virus induces large syncytium formation in primary human small airway epithelial cells by a SLAM(CD150)-independent mechanism. Virus Res. **94**:11–16.
69. **Tatsuo, H., N. Ono, K. Tanaka, and Y. Yanagi.** 2000. SLAM (CDw150) is a cellular receptor for measles virus. Nature **406**:893–897.
70. **Thormar, H., K. Arnesen, and P. D. Mehta.** 1977. Encephalitis in ferrets caused by a nonproductive strain of measles virus (D.R.) isolated from patient with subacute sclerosing panencephalitis. J. Infect. Dis. **136**:229–238.

Journal of Virological Methods 168 (2010) 267–271

Contents lists available at ScienceDirect

Journal of Virological Methods

journal homepage: www.elsevier.com/locate/jviromet

Short communication

Development of a novel TaqMan real-time PCR assay for detecting rubella virus RNA

Kiyoko Okamoto*, Kaoru Fujii, Katsuhiro Komase

Laboratory of Rubella, Department of Virology III, National Institute of Infectious Diseases, Murayama Branch 4-7-1 Gakuen, Musashimurayama, Tokyo 208-0011, Japan

Article history:
Received 8 January 2010
Received in revised form 18 May 2010
Accepted 25 May 2010
Available online 1 June 2010

Keywords:
Rubella
Diagnosis
TaqMan
RT-PCR

ABSTRACT

Although the number of cases of rubella and congenital rubella syndrome has decreased recently in Japan, both are still important health problems. To control rubella infection, a rapid and reliable method for diagnosis of rubella is required as soon as possible. Direct detection of the viral genome in clinical samples is viewed as crucial for laboratory diagnosis. In this study, a novel diagnostic method for rubella virus, based on a fluorogenic real-time PCR (TaqMan) assay, was developed, and its sensitivity for various virus strains was compared with that of a conventional RT-PCR. The new assay allowed more rapid and sensitive detection of the virus than did the conventional RT-PCR, and could detect at least 10 pfu of the native strains in Japan (1a, 1D, 1j).

Rubella is caused by infection with *Rubella virus* (RV), and the symptoms include a mild rash and a fever. The most severe effect of RV infection is the congenital rubella syndrome (CRS), which is caused by infection during early pregnancy and may result in abortion, miscarriage, stillbirth, and severe birth defects. The most common congenital defects are sensorineural deafness, heart disease, and cataracts. RV belongs to the genus *Rubivirus*, family *Togaviridae*, and possesses a positive-sense, single-stranded RNA with a 9.8-kb nucleotide length that contains two open reading frames (ORFs). The 5′- and 3′-ORFs encode the nonstructural proteins p150 and p90 (Liang and Gillam, 2000; Pugachev et al., 1997) and the structural protein capsid, E1 and E2, respectively (Frey, 1994; Oker-Blom et al., 1984; Yao et al., 1998).

In Japan, single-dose rubella vaccination was started in 1976, and two-dose vaccination against measles and rubella by a combined Measles and Rubella (MR) vaccine was introduced in 2006. In 2008, a national vaccination campaign to control measles and rubella was introduced, with the aim of eliminating measles and decreasing rubella by the year 2012. To support this effectively, an active surveillance system including a rapid and reliable method for laboratory confirmation is essential. Current laboratory diagnosis employs mainly serological methods that measure anti-rubella IgM, although it takes at least 5 days after the onset of infection to detect a specific increase in anti-rubella IgM. Detection of viral RNA, for example, in oral fluid, is possible by RT-PCR if samples are obtained during the first 4–5 days after the onset of a rash (CDC, 2008). Rubella symptoms are similar to those of other viral infections (e.g. measles virus, echovirus, or parvovirus B19), making it difficult to differentiate rubella from other viral infections on the basis of clinical symptoms alone (WHO, 2007a). Other viruses such as measles and parvovirus B19 sometimes give rise to false-positive IgM results (Tipples et al., 2004).

Therefore, detection of the RV genome is considered to be a promising approach for monitoring rubella because of its sensitivity and specificity. Although several RT-PCR assays for the detection of the RV genome in clinical specimens have been described (Cooray et al., 2006; Jin and Thomas, 2007; Vyse and Jin, 2002; Zhu et al., 2007), the conventional methods require a long time and multiple procedures, and are susceptible to carry-over contamination when multiple samples, including positive samples, are tested. Real-time PCR does not require post-PCR sample handling and seems to be more feasible for much faster and higher-throughput assays. Although some investigators have described real-time PCR methods for detecting the RV genome (Abernathy et al., 2009; Hübschen et al., 2008; Rajasundari et al., 2008; Zhao et al., 2006), there has been no report confirming the sensitivity and specificity between various viral strains, or excluding the possibility of false-positive results for other viruses exhibiting similar symptoms. In this study, a novel real-time PCR system that included one-step RT-PCR for the diagnosis of rubella infection was developed and the sensitivity was compared with that of a conventional nested RT-PCR, which covers the sequencing region for genotyping, using synthesized RNA and various virus strains. This system permits detection of a minimum of 10 copies of a positive control RNA and 1 pfu of RV.

Twenty-six complete sequences of RV accessible on GenBank were aligned, and a highly conserved region was selected in design-

* Corresponding author. Tel.: +81 42 561 0771; fax: +81 42 561 1960.
E-mail address: k-okmt@nih.go.jp (K. Okamoto).

0166-0934/$ – see front matter © 2010 Elsevier B.V. All rights reserved.
doi:10.1016/j.jviromet.2010.05.016